Nuclear Physics Laboratory Manual

June 28, 2016

1 Experiments Using Geiger-Müller Counter

Detectors are the most essential and important constituents of all nuclear radiation counting systems. In common laboratory experiments generally radioactive sources are used as a source of radiations on which measurements are conducted. During disintegration, radioactive sources emit α-, β- and γ- radiations and also x-rays through secondary processes. The α- and β- radiations are charged particles while x- and γ-rays are photons. These radiations are detected in experiments from which information on their energies, intensities, etc. are obtained. Thus, a detector should be able to count particles and quanta one by one as they are incident on it.

Fundamentally, the process of detection proceeds through interaction of a given type of radiation with the material medium which constitutes the active volume of the detector. A detector can be made from either a gas, a liquid or a solid to serve as the active medium. In the following section we will discuss only about gas detectors. The most common gas based detectors are ionisation chambers, proportional and Geiger-Müller (G.M.) counters.

1.1 Geiger-Müller Counter

A G.M. counter is an example of a gas based counter. It is based on ionisations produced by a charged/uncharged energetic particle in matter. Charged particles such as α, β, etc., directly ionise the gas used to fill up the counter volume. Radiations like x- and γ-rays produce secondary electrons which in turn produce ionisation.

An ionising particle, while passing through the gas in the counter, collides with the gas atoms producing ionisation in its wake. If the volume of the gas is adequately large, the particle will go on losing its energy by producing ions and eventually come to a stop within that volume. On an average $\simeq$ 30 eV is spent per ionisation event. Thus one ionising nuclear particle leaves behind a number of ion pairs called the primary ions. Since the process of ion production becomes complete in a short time of a few microseconds, a burst of both positive and negative charges is generated. These charges are swept away by an applied electric field, and get collected on the respective electrodes. Each burst, if measured by a suitable instrument, will count the particle.

In a most common type of gas-filled counter, there is a cylindrical cathode (1 - 2 cm diameter) and an axial anode made from a fine tungsten wire (15 - 100 μm in diameter) as shown in Fig. 1.1. Generally, it is filled up with a noble gas (say, argon) at nearly 100 Torr pressure.

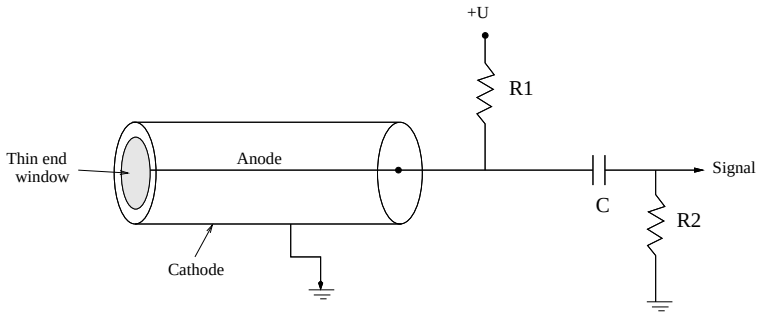

Figure 1.1: Schematic diagram of a gas-filled counter

A positive voltage (+U Volts) is applied to the anode wire via a high resistance R1 and the cylindrical cathode is held at ground potential. Alternatively, a negative voltage could be applied to the cathode and the anode grounded via R2.

A charged particle, on entering the counter, ionises the gas atoms to produce, along its path, as many electrons as positive ions. The number of them, though statistical in nature, is determined by the quantity of energy the incident particle deposits within the counter. The electrons created by ionisation in the gaseous medium then move towards the anode wire while the positive ions towards the cathode. The charge $\delta Q = ne$, where n is the number of ions formed and e is electronic charge, is thus collected at the anode and will charge the counter capacity C to a potential $\delta V = \delta Q/C$. The electrons move faster than the much heavier positive ions. Hence, the electrons reach the anode in a short time while the ions are still on their way to the cathode.

The electric field E_r at a distance r from the axis of the central wire arising from the applied potential difference U between the anode and the cathode under cylindrical symmetry is

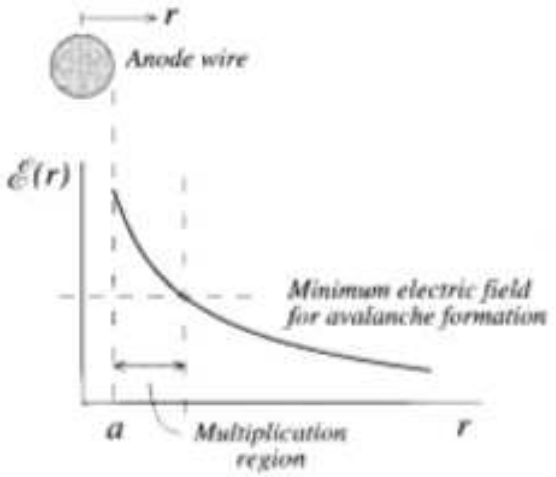

Figure 1.2: Electric field strength as a function of distance from the anode wire of GM detector.

$$\mathcal{E}_r = \frac{U}{r\ ln\left(\frac{b}{a}\right)}$$

where a is radius of the anode wire and b is radius of the cathode cylinder.

It is seen from this expression that at points close to the anode wire the field is very high (see Fig. 1.2). For example, for $U = 10$ Volts, $b = 1$ cm, $a = 0.003$ cm and $r = 0.01$ cm (i.e., r is 0.007 mm away from the surface of the anode wire), $\mathcal{E}_r = 172$ Volts/cm and for $U = 500$ Volts, $\mathcal{E}_r = 8.6 \times 10^3$ Volts/cm. We will see later that such a high electric field near the anode wire has important role on the performance characteristics of this type of counter.

1.1.1 Characteristics of a gas filled counter

We will discuss the case of a gas filled counter in which the electrodes have a cylindrical configuration as shown in Fig. 1.1. The characteristics of such a counter defines its operational behaviour as a function of the applied voltage U across it.

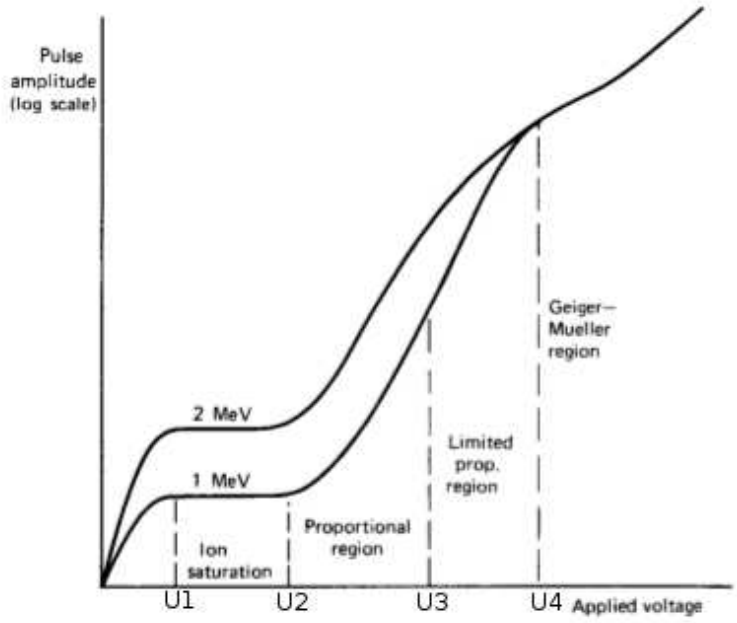

Figure 1.3: Pulse height variation of gas-filled detector with applied voltage

Study of the characteristics of a counter is essentially related to the manner in which the charge produced by the ionising radiation in the counter volume is collected by the electrodes. Let us consider, for example, the case of a stream of α-particles of energy $E = 1$ MeV. Each particle, in this case, produces, on an average, the same number of primary ion pairs in the sensitive volume of such a counter. The curve of Fig. 1.3 can now be drawn for a counter (having given electrode dimensions, the type of filling gas and the gas pressure) by plotting the charge collected by the capacitor (C) as a function of the potential difference U applied

across the counter electrodes. The two curves shown are drawn for incident α-particles of energies $E = 1$ MeV and $E = 2$ MeV. For convenience of discussion these curves are broadly divided into five regions marked in Fig. 1.3 by dashed vertical lines. Note that the positions of these boundary lines are approximate since the curves do not show any sharp change in slope across them. It is assumed that all the particles dissipate their entire energy within the counter volume.

Region A : (U= 0 to $U1$ ***Volts)***

At very low voltages a number of the primary ions formed readily recombine with the electrons since they are not capable of gaining sufficient energy from the field to avert recombination. The amount of charge Q collected on C is thus less than that carried by all the primary ion pairs together. However, Q increases with U as more and more ion pairs are collected at respective electrodes..

Region B : ($U1 < U < U2$***), Q is same for incident radiation of any given energy***

In this region, the primary ions and electrons acquire just enough energy to avoid recombination. Hence, all of them can now move up to the respective electrode to deposit the entire charge generated during formation of primary ions on capacitor C. Such a condition prevails in an ionisation chamber and accordingly, the region B is called the *ionisation chamber region*. In a typical case, a 5 MeV α-particle will produce an output pulse amplitude V ~ 0.5 mV on a total output capacity of 100 pF.

Region C : ($U2 < U < U3$***, Q increases rapidly with U)***

As the applied potential U is increased to move into this region, a new phenomenon starts. The primary ions now acquire enough energy (particularly near the anode wire where the electric field is high) between successive collisions with the gas atoms to initiate fresh ionisation. The secondary ions so formed will also, in their turn, take part in the process to eventually build up a large number of ion pairs. This is thus an internal ion multiplication process which is strongly dependent on the applied potential U. The number of times the ions get multiplied is called the gas multiplication factor m. The value of m may be as large as 10^4 . Furthermore, in this region the factor m is proportional to U. Hence, for a given U in this region, the pulse amplitude delivered at the anode of the counter is proportional to the number of primary ions, i.e., on the energy of the incident particle. The region C is known as the proportional region and a counter operated in this region is called a proportional counter. For higher energy particle, the number of primary ions is larger. Hence the curve for $E = 2$ MeV lies above the $E = 1$ MeV in Fig. 1.3 for the regions B and C.

From the above discussion we find that a counter operated in either B or C region behaves as a proportional device which not only detects nuclear radiations but also enables measurement of their energies. However, in laboratory experiments a proportional counter is favoured over a ionisation chamber because they are capable of delivering much larger pulses (for an incident α-particle of energy 5 MeV, output pulse of one Volt or so in amplitude is not difficult to obtain). Note that a large pulse can be processed and recorded more easily than a smaller one.

Region D ($U3 < U < U4$***, Q increases with U disproportionately for the incident particles of different energies)***

This region is called a region of limited proportionality. Here, the multiplication factor m progressively loses its proportional behaviour as U is increased and, hence, a counter operated in this region is not suitable for energy measurement. At $U = U4$, Q becomes same for all incident energies and types of particle.

Region E *($U > U4$,* ***Q is very large and same and independent of radiation type and energy)***

At any U in this region, the ions acquire large energy such that gas multiplication advances to a stage of avalanche formation even if a single primary ion pair is formed. The values of m shoots up to $\sim 10^9$ and neither the type nor the energy of the incident particle has any bearing on the size of the charge pulse (Q) produced at the output electrode. The ions and electrons in such circumstance spread quickly all along the anode wire and thoroughly surround it. The electrons are then collected at the anode within a short time while the ions, as usual, have started moving towards the cathode cylinder. The region is known as the Geiger region and a counter operated in this region is called a Geiger Müller or simply a G.M. counter.

Obviously in this case, pulses obtained from a G.M. counter is quite large (several Volts) and have identical shape and amplitude for incident radiations (particles and photons) of all descriptions and energies. A G.M. counter can therefore be used only to detect and count radiation but is neither suitable for use in particle identification nor in measuring their energies.

1.1.2 Quenching of discharge in a G.M. counter

The course of events that lead to production of a pulse in a G.M. counter do not appear to be as simple as the above picture describes it. The electrons produced in the avalanche created in the vicinity of the anode wire, get collected in $\sim 1\mu$s while the ions, being about 100 times less mobile, stay around the central wire in the form of a positive charge sheath for some-time. This sheath reduces the field around the wire and causes the avalanche to stop. As the ions reach near the cathode (in $\sim 10^{-4}$ sec) they pull electrons from there to become neutral. The resulting gas molecules, are consequently raised to excited states which deexcite shortly thereafter by emission of radiation. There will always be some ultraviolet content in these radiations causing photoelectric emission from the cathode surface. These photoelectrons initiate a fresh avalanche process. The same sequence of events repeats to give rise to recurrent avalanches leading to production of a chain of pulses, a situation resembling that created by a continuous discharge in the counter. Such a situation is undesirable and the sequence of avalanche has to be stopped after the first one. The process by employing which the entire event is kept restrained to only one avalanche formation per incident particle following formation of the primary ions is known as *quenching*.

Quenching can be achieved in two ways. The external nonself-quenching technique requires a circuit arrangement which momentarily reduces the potential applied to the anode immediately after arrival of the first avalanche of electrons on it. As a result the electric field reduces to a value too low for formation of a second avalanche. In practice this technique is not useful and therefore, it will not be discussed further.

To implement self-quenching in a G.M. counter it is filled up with a mixture of 90% argon (argon, a noble gas, is most commonly used) and 10% dehydrated vapour of ethyl alcohol or any other suitable polyatomic organic vapour. No external quenching circuit is necessary in this case. This organic vapour serves as the quenching agent.

In such a counter, both argon and alcohol molecules take part in avalanche formation and, hence, the positive ion cloud contains both kinds of ions. The ionisation potential of argon is 15.7 eV whereas that of alcohol is 11.3 eV. As these two kinds of ions move towards the cathode they collide with each other. The higher ionisation potential of argon makes it possible for its ions to become neutral atoms by extracting electrons from the alcohol molecules. The reverse can not take place. Again the ions may suffer as many as 10^5 collisions before reaching the cathode surface. Hence, the ion cloud reaching the cathode almost entirely contains alcohol ions.

These alcohol ions will now pull electrons from the cathode surface to become neutral and in doing so many of them will acquire some energy. Since large polyatomic organic molecules of alcohol favour dissociation to excitation, this excess energy does not take the polyatomic molecule to an excited state but causes its dissociation into simpler ones. No UV or other radiations are emitted in the process and hence a second avalanche mechanism can not start. In other words, the discharge is quenched. Initially there are about 10^{20} alcohol molecules in a counter and in each avalanche 10^{10} get dissociated, i.e., spent up. Thus the useful life of a G.M. counter is about 10^{10} counts.

We have another point to consider. An energy excess of 4.4 eV (=15.7-11.3, released when an Ar^- atom neutralizes itself) is radiated as UV light which is likely to initiate a second avalanche. However, alcohol or similar polyatomic molecules have a strong absorption band in the same wavelength region where the UV light is absorbed causing dissociation of the molecule rather than excitation and a second avalanche can not start.

Halogens can also be used as quenching gases. Of them chlorine and bromine have been found to be most suitable. The diatomic molecules of a halogen dissociate as in the case of alcohol into atoms to make quenching effective. But unlike alcohol, the atoms recombine to form back the molecules again. As a result the quenching gas is not consumed and the counter has a virtually unlimited life.

1.1.3 Characteristics of a G.M. counter

A counter meant to be operated in the G.M. region (region E, also see Fig. 1.3) is generally filled up with a mixture of Argon gas and alcohol vapour to partial pressures of $\sim$ 9 cm and 1 cm of Hg at room temperature, respectively. A typical characteristic curve presented in Fig. 1.4 shows the operating characteristics of such a counter.

Before we discuss the nature of this characteristic curve, we should remember that some electronic instrument assembly has to be used with the counter to count its pulses. These instrument assembly has an inherent threshold bias which a counter pulse has to overcome in order to be recognized and registered as a count. The counter setup begins to register counts when a potential U_{Th} called the G.M. counter threshold potential is applied. Below U_{Th} the counter behaves as an ionisation chamber and the corresponding output pulses are

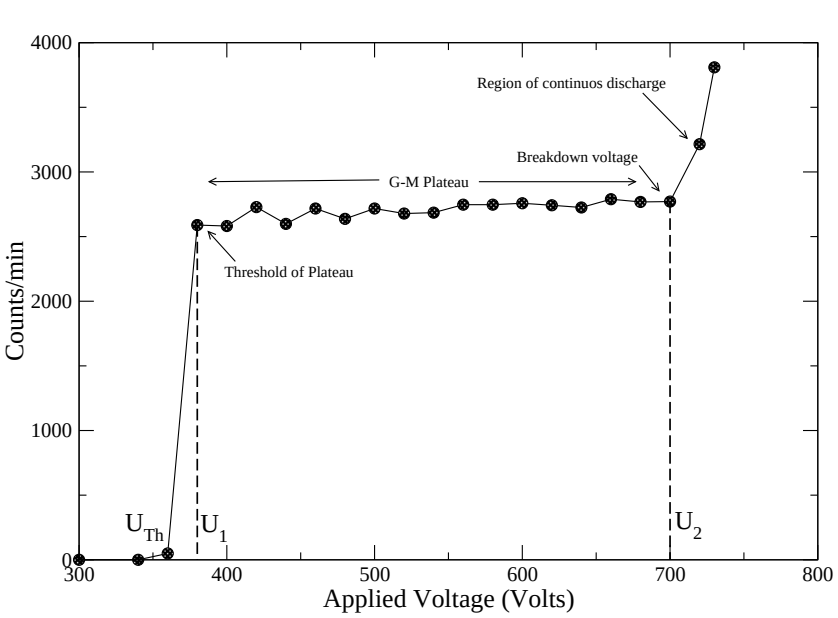

Figure 1.4: Plateau characteristics of a GM counter.

too small to overcome the threshold bias; hence, they are not recorded.

In the region U_1 to U_2, called the plateau region, the count rate is nearly constant. This is also called the Geiger region (G.M. region) discussed earlier. The applied voltage at which this region starts (U_{Th}) in Fig. 1.4) is the Geiger threshold. The constancy of count rate over the plateau is advantageous because the count rate is almost independent of the applied voltage U. The region shows a slightly upward slope with increase in U. The reason possibly lies in the occurrence of occasional secondary unquenched discharges in the tube as U is increased. The counter operated at $U > U_2$ produces continuous discharge for which it is rendered unsuitable for use as a counter for detecting any incident radiation.

The output pulse amplitude obtained from the counter operated in the G.M. region is determined by the difference (U_{op}- U_{Th}). To achieve a condition of noncritical operation a long plateau is obviously desirable. The slope of plateau remains within 1% per 100 volts of applied potential. The length and slope of the plateau depend on the nature of the filling gas, the condition of the anode wire and the condition of the cylinder surface.

Although all G.M. counters work on the same basic principle, their constructions are different. A counter has to be trimmed to suit the application for which it is meant. A G.M. counter intended to detect β-particles has to have a thin entrance window to admit low energy β-particles. A 1 mg cm^{-2} thick mylar window admits all electrons of energy > 20 keV into the counter volume. In these counters, it is convenient to fix the window at one end when it is called an end-window counter (Fig. 1.5). For detecting γ-rays on the other hand, a much thicker window can be tolerated except when detection of very low energy γ-rays is concerned. In this case, the size of the counter need be made large enough so that the γ-rays can undergo adequate number of interactions in the available counter volume. These counters can be both end-window as well as common types.

Figure 1.5: A common type GM counter

For heavier charged particles such as alpha the window has to be very thin. Windowless continuous gas flow type counters are recommended for use in this case.

1.2 EXPERIMENT 1 : Characteristics of Geiger Müller Counter

1.2.1 PART I : Operating Plateau for the Geiger Tube

Apparatus

1. Geiger-Müller counter
2. High Voltage Bias supply
3. Timer and Counter
4. Cables
5. Digital Storage Oscilloscope (DSO)

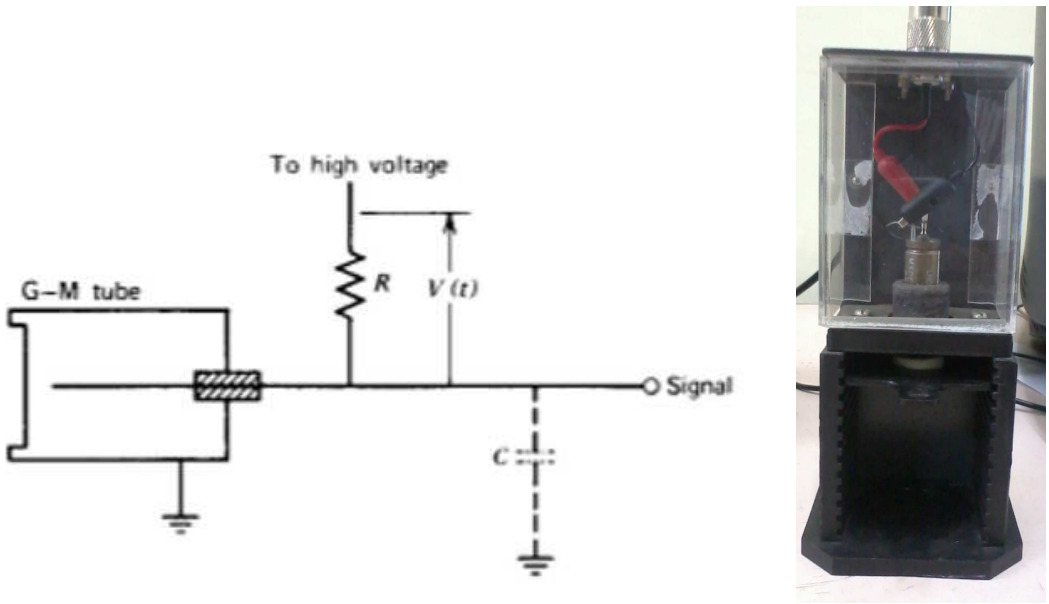

Figure 1.6: Schematic diagram of a gas-filled counter. A snap of the detector setup is also shown.

Purpose

1. To determine the voltage plateau for the Geiger tube and to establish a reasonable operating point for the tube.

2. We are going to inspect pulses as obtained from the counter. In the first part of the experiment we will study how pulse height increases with increasing applied voltage. In the second part of the experiment estimation of dead time, resolving time and recovery time of the counter will be made.

Procedure

The Schematic diagram of a GM counter is shown in Fig. 1.6. For a typical Geiger tube that has an operating point in the vicinity of 550 V, a counts vs. voltage curve is displayed in Fig.1.7. The region between R_1 and R_2, corresponding to operating voltages V_1 and V_2, is called the Geiger plateau region. Voltages $> V_2$ in Fig. 1.7 cause a continuous discharge in the tube and should be avoided, because a continuous discharge will definitely shorten the life of the tube.

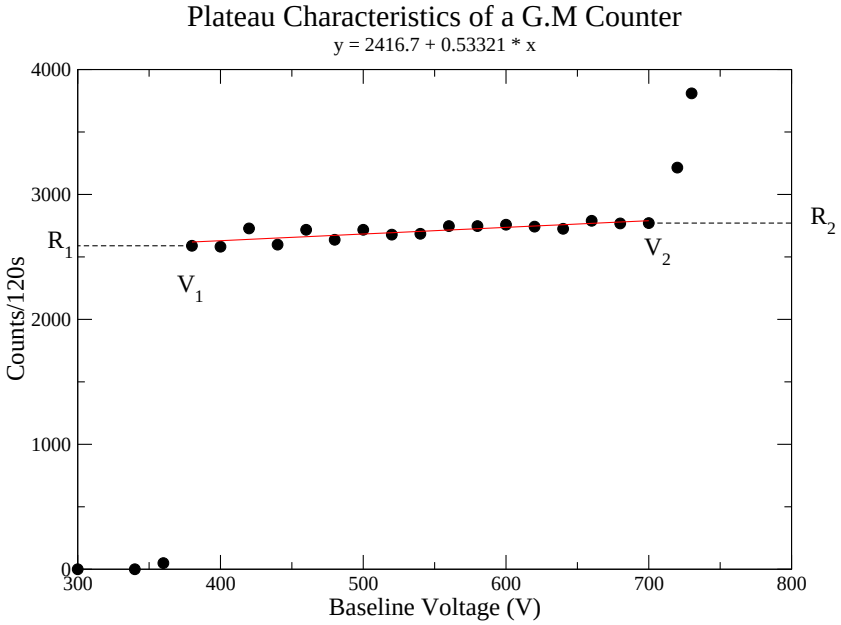

Figure 1.7: Plateau characteristics of a GM counter. R_1 and R_2 are the count rates at V_1 and V_2 voltages, respectively.

1. Inspect and identify every component part of the G.M. counter assembly you are going to use.

2. Ensure that all power is turned off. Set up the electronics as shown in Fig. 1.6.

3. Make sure that the H.V. supply knob is at the minimum level.

4. Switch on the power supply of the Electronic box.

5. Gradually increase the H.V. bias supply in steps of 50 V (say) until the counter just begins registering counts. This point is called as the starting voltage (shown as V_1 in Fig. 1.7). Starting voltages are in the range of 300 - 350 V.

6. Put a β- or a γ-source at a distance of ~ 5 cm from the counter.

7. Reset the counter. Set the timer section for 20 sec. time intervals (say), and count for 20 seconds. Record the number of counts.

8. Increase the high voltage by 30 V (say) and count again for 20 seconds. Record the number of counts in the following table.

Table 1.1: Data for Plateau characteristic of the GM counter.

High Voltage (V)	Counts
300	
330	
360	
390	
420	
.	

9. As you proceed, you will find a voltage region where the count rate is nearly the same. This is the plateau region beyond which the count rate increases sharply. The H.V. at which such a sharp change in count rate is observed (the region beyond V_2 of Fig. 1.7) corresponds to onset of discharge in the counter gas and a further increase in H.V. will take the counter to the continuous discharge region. **Immediately decrease the H.V. to bring the counter back to normal operating condition.**

   CAUTION !!!: If operated in the discharge region for a minute or more, a counter may suffer from an irreversible damage.

10. Plot the recorded counts/sec vs. applied (Baseline) voltage and draw a curve. It should look like the one of Fig. 1.7.

11. Mark the various regions on the graph and indicate the operating voltage for your counter. The operating voltage is $V = (V_1 + V_2)/2$.

12. Evaluate your Geiger tube by measuring the slope of the plateau in the graph. The slope of the plateau is defined as:

$$\text{Slope (in \% per 100V)} = \frac{R_2 - R_1}{R_1} . \frac{100}{V_2 - V_1} \times 100\%$$

    Here, R_1 and R_2 are the count rates at voltage V_1 and V_2, respectively. Record the operating voltage selected for use in the remainder of the experiments.

Exercises

1. The best operating voltage for the tube = ———————— Volts.

2. Will this value be the same for all the different tubes in the lab?

3. Will this value be the same for this tube ten years from now?

4. How can you explain the slope of the plateau region?

5. Why there is a sharp increase in count beyond region V_2?

6. How does the avalanche process of gas ionisation stop in the GM tube?

1.2.2 PART II : Analysis of Signal pulses from GM counter

Procedure

A snapshot of GM pulses as viewed on DSO screen is shown in Fig. 1.8.

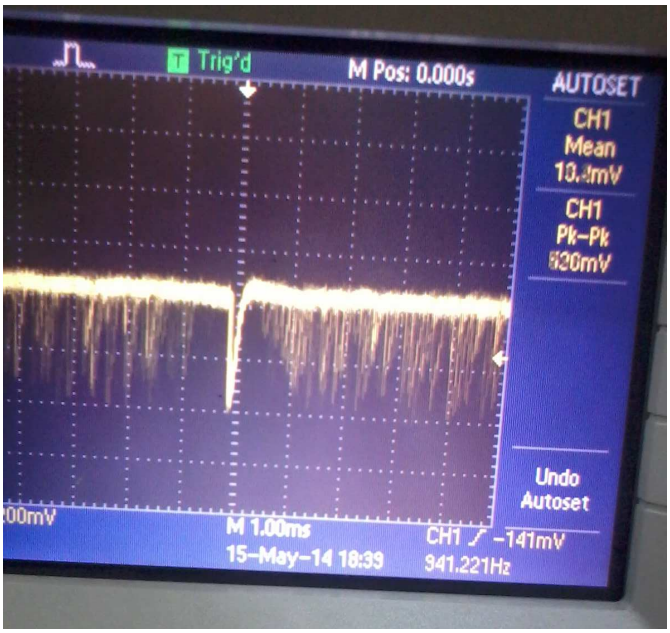

Figure 1.8: Pulses from a GM detector as seen on DSO screen.

(A) Variation of pulse height with increasing High Voltage

1. Set the G.M. counter into operation (see Expt in 1.2). Apply High Voltage such that the counter begins to count (say 300 or 350 V).

2. Connect a Digital Storage Oscilloscope (DSO) to see the signal pulses from G.M. counter. Trigger the DSO to see a full pulse on the screen (see Fig. 1.9).

3. Measure the pulse height in Volt using cursor. Increase the HV in steps of 50 V in the Plateau region and measure each time the height of GM pulse and fill the following table.

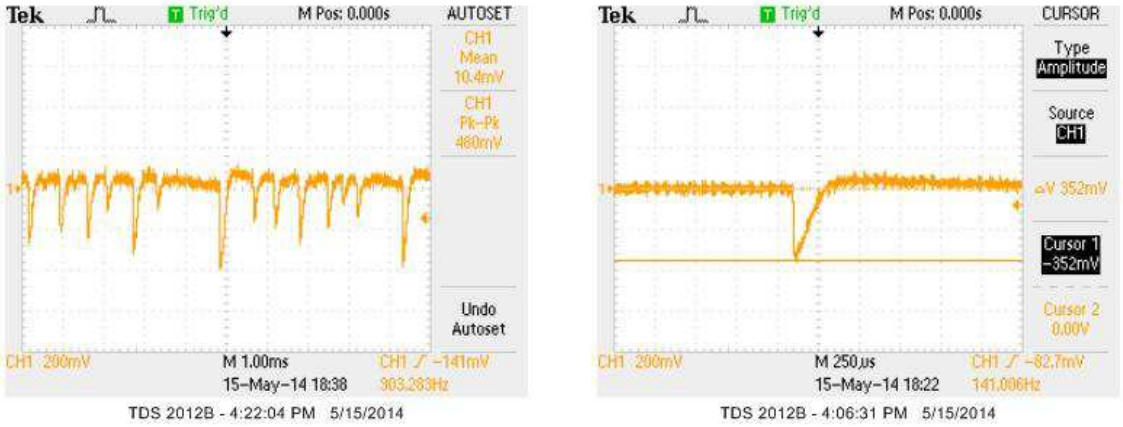

Figure 1.9: Oscilloscopic view of G.M. counter output pulses coming at a large rate. Note the overlapping of pulses.

Table 1.2: Variation of pulse height with high voltage applied to GM counter.

High Voltage (V)	Pulse height (Volt)
300	
350	
400	
.	
.	
.	

4. Plot the data (pulse height vs High Voltage), as shown in Fig. 1.10.

(B) Visual measurement of dead time, resolving time and recovery time

1. Set the G.M. counter into operation. Use the operating voltage determined in the first Experiment (see 1.2) for its operation.

2. Connect a Digital Storage Oscilloscope (DSO) to see the signal pulses from the G.M. counter. Meanwhile record the counts with a scaler by placing a source at such a distance from the counter such that a count rate as large as 100 counts/sec is recorded. The pulses in the oscilloscope will look like the one shown in Fig. 1.9.

   The time interval defined by the start of the main pulse and the end of the pulse is the dead time τ. No other pulse can appear within this interval. The counter setup can therefore record counts after τ. The resolving time is the time interval between start of a pulse of full height and a pulse of small height adjacent to the full-height pulse. The recovery time τ_R shown in Fig. 1.11 is the time the counter takes to regain its quiescent condition becoming again capable of delivering a pulse of full size.

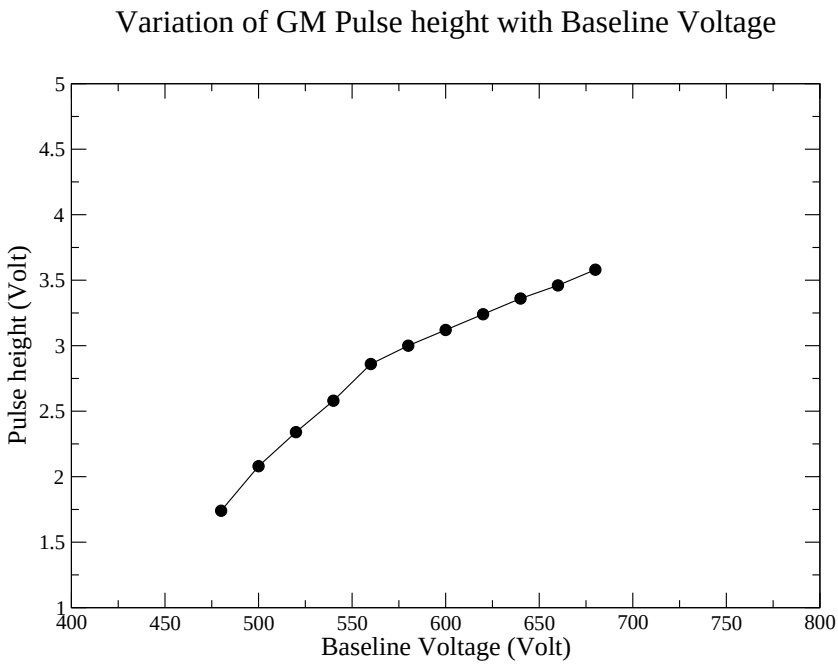

Figure 1.10: Pulse height of a GM counter with applied high voltage

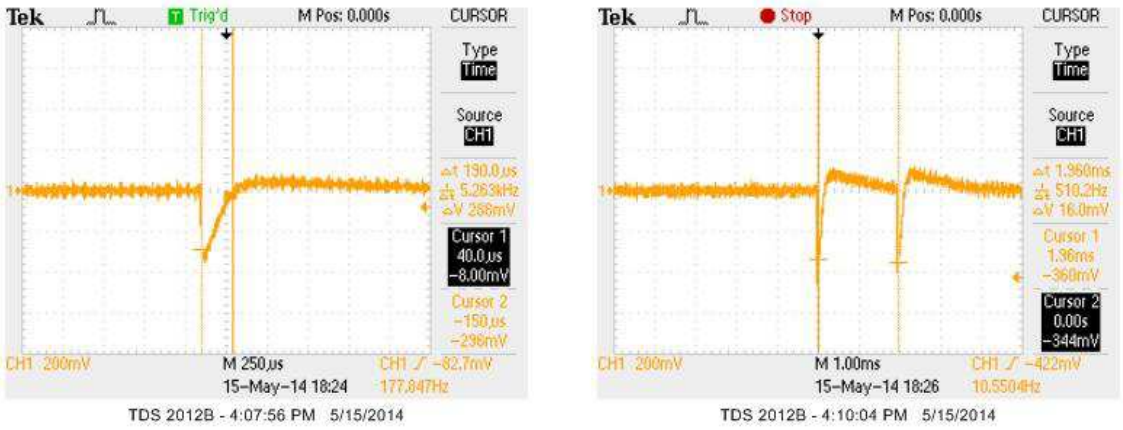

Figure 1.11: Demonstration of dead time and recovery time of a G.M. counter.

3. Take a snap of pulses appearing on the screen of the DSO. Measure time separation between two pulses and keep record of the data.

4. Repeat the process several times (say 20 times) and keep the record of data sets in a table.

   The minimum separation between two full-height pulses will be the recovery time. The minimum separation between a pulse of full height and a adjacent pulse of smaller height will give you an estimate of resolving time of the detector.

Exercises

a. Why does the pulse height increases with increasing voltage?

b. Do you see any change in dead time of detector with increasing voltage?

c. Using the oscilloscope, determine the minimum observable time between the leading edge of successive pulses.

d. How pulses of smaller height are formed?

1.3 EXPERIMENT - 2 : Measurement of dead-time of a GM Counter

1.3.1 Purpose

1. We would like to determine dead-time of G.M. counter using double source.

2. The measured deadtime can be compared with the value obtained in Expt. 1 using visual method.

1.3.2 Relevant Information

The Geiger counter is very slow in responding to detected events. It takes of the order of a microsecond for the detector to develop its full response to the incident gamma-ray or charged particle, and it requires hundreds of microseconds to restore the detector to full sensitivity for the next event. The strict definition of the dead time of the Geiger counter is the time from initial response to a detected event until the detector can exhibit the earliest response to a subsequent event. But, the electronics processing the Geiger tube output pulses has a fixed voltage threshold that the pulses must exceed to be counted. Thus, the resolving time includes the previously defined dead time, but adds the time it takes for subsequent pulses to recover to a sufficient amplitude to cross the discriminator threshold and be counted. In practice, the distinction between dead time and resolving time is often blurred, and the resolving time is frequently labeled as the dead time. That is a pragmatically empirical convention, because the measurement of counting rate is always made after the supporting electronics has added its contribution to the dead time.

The large dead time of the Geiger counter distorts the measured counting rate for counting rates above 5000 counts/minute. Thus, it is usually necessary to make a dead-time correction to obtain the true counting rate. Usually, the measurement of the dead time is accomplished with a split source. However, since we do not have split source in the lab, we will use two circular disk sources for the same purpose.

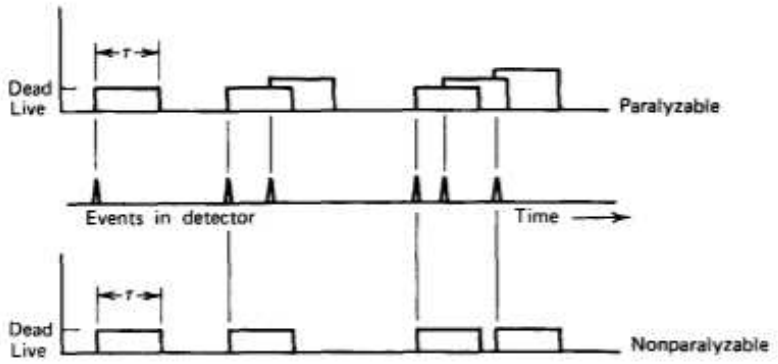

Figure 1.12: Illustration of two assumed models of dead time behaviour for radiation detector.

The dead time of a nuclear radiation counting system is typically dominated by one of two types of dead time: (i) paralyzable (extending) dead time, or (ii) non-paralyzable (non-extending) dead time. The fundamental assumptions of the models are illustrated in Fig. 1.12. Six randomly spaced events are shown at the middle part of the figure. At the lower part of the figure the dead time behavior of a detector is shown within the non-paralyzable model. A fixed time interval τ is assumed to follow each true event. The true events that occurs during the dead period of the detector are lost and the detector would record four counts from the six true events. In contrast, the behavior of a paralyzable detector is shown at the upper panel of Fig. 1.12. The same dead time τ is assumed to follow each true interaction. In this case also the true events that occur during the dead period of the detector are not recorded as counts. However, the dead time is extended by another period τ following the lost event. In the example, only three counts are recorded for the six true events.

The losses predicted by the above two models are nearly same and differ only when true event rates are high. These models presents two extremes of idealized system behavior, and real counting systems will often display a behavior that is intermediate between these extremes.

The dead time contributed by the Geiger counter is reasonably accurately modeled as a non-paralyzable dead time. The measured counting rate, R, is related to the true counting rate, r, at the input to the detector

$$R = \frac{r}{1 + r.T_d} \tag{1.1}$$

Here, T_d is the dead time caused by each quantum of radiation that is detected when the counter is free to accept a new event. Note that the dead time reduces the measured counting rate relative to the true counting rate, and higher counting rates cause a greater relative reduction.

In practice, the experimenter only has access to the measured counting rate, R, after dead time losses have occurred. Consequently, it is important to calculate the true counting rate,

and this requires knowing the dead time per pulse, T_d. Using equation 1.1, we can write the true counting rate from the measured counting rate and the known dead time per pulse.

$$r = \frac{R}{1 - R.T_d} \tag{1.2}$$

Another useful way to express the information in equations 1.1 and 1.2 is the percent dead time loss:

$$\text{Percent Dead Time} = \frac{r - R}{r} \times 100\% = R.T_d \times 100\% = \frac{r.T_d}{1 + r.T_d} \times 100\% \tag{1.3}$$

One way to measure the dead time per pulse, T_d, would be to observe the output of the GM counter on the oscilloscope and determine the minimum spacing between the leading edges of two successive pulses (See Experiment in 1.2.2). Because the arrival times of the pulses are randomly distributed in time, this method requires a fairly high counting rate to make it easy to find the minimum pulse spacing.

The double source method is another technique to measure the dead time of GM counter. Usually, a split source, a circular disk source splitted into two half, is used in the measurement process. However, due to unavailiblity of the source we will follow the process using two circular radioactive sources.

First, place the two sources side by side so that both the sources are equally visible by the GM counter. Adjust the distance between the source and the counter to achieve a percent dead time in the range of 10% to 20%. For a 100-μs dead time, this implies measured counting rates in the range of 1,000 to 2,000 counts/s, or 60,000 to 120,000 counts per minute.

Next, one the source (first) is removed, and the counting rate of the other one, R_2, is measured. Subsequently, the first one is carefully reinstalled without disturbing the second source, and the counting rate from the pair of sources, R_{12}, is measured. Finally, the second source disk is removed without disturbing the first source, and the counting rate, R_1, is measured. R_1, R_2, and R_{12} can be inserted into equation 1.2 to write the equations for r_1, r_2, and r_{12}, respectively. Because of the dead time, $R_{12} < (R_1 + R_2)$. But for the true counting rates

$$r_{12} = r_1 + r_2 \tag{1.4}$$

Combining equation 1.4 with the expressions for r_1, r_2 and r_{12} from equation 1.2, permits solving for T_d in terms of the measured counting rates. The exact solution for the case of zero background is (see the book by G.F. Knoll)

$$T_d = \frac{R_1 R_2 - \left[R_1 R_2 \left(R_{12} - R_1\right)\left(R_{12} - R_2\right)\right]^{1/2}}{R_1 R_2 R_{12}} \tag{1.5}$$

An approximate solution that is sometimes employed is

$$T_d \simeq \frac{R_1 + R_2 - R_{12}}{2 R_1 R_2} \tag{1.6}$$

1.3.3 Procedure

1. Set the G.M. counter into operation (see Expt. in 1.2). Set the High Voltage knob to the operating voltage of the tube. Take two ^{90}Sr sources of reasonable activity.

2. Place both the radioactive source disks (source window in upward position) on the sample-holder shelf, with the touching point of the disks centered below the Geiger counter window. Set the Timer and Counter for a 1-minute counting interval

3. Measure the counts for 1 minute.

4. If the number of counts in step 3 is not between 10,000 and 20,000, adjust the source to detector distance to bring the counting rate within that range.

5. Remove one of the source (the left one) and make a 1-minute count on the other source (the right one). Record the count. Define this count to be R_1.

Table 1.3: Data for determination of dead time of the G-M counter

Sr. No.	Count rate for Source 1 (R_1)	Count rate for Source 2 (R_2)	Count rate for combined source (R_{12})	Dead time (T_d)	Avg. Dead Time
1					
2					
3					
4					
5					

6. Being careful not to disturb the right source, place the left source alongside the right one and make a 1-minute count. Define this count to be R_{12}.

7. Being careful not to disturb the left source, remove the right source and count the left source for 1 minute. Define this count to be R_2.

8. Calculate the dead time of the Geiger tube via equation 1.5. The answer should be in minutes/count. Because counts are often considered a dimensionless number, the dead time can also be expressed simply in minutes or seconds.

   The dead time established in step 8 should be used to correct all measured counting rates via equation 1.2 whenever the percent dead time exceeds 1%.

9. You can repeat the steps 2-8 for five times and take an average of the measured T_d values.

1.3.4 Exercises

a. Calculate the value of T_d from equation 1.6 and compare it to the result from equation 1.5. What is the percent error in the approximate result from equation

1.6 compared to the more exact result from equation 1.5?

b. Based on equation 1.3, what is the measured counting rate that will correspond to a 1% dead time? Correct all subsequent measurements above that counting rate for the dead time loss.

c. Considering the apparatus and procedures employed in this measurement, what are the most important sources of error in measuring T_d?

d. What is the percent difference between the values of dead time measured in Expts 1.2.2 and 1.3.?

e. Using the approximate formula for T_d (equation 1.6) calculate error in your measured T_d value using error propagation rule (see book by G.F. Knoll). What will be the error in the average value of T_d?

1.4 EXPERIMENT 3 : Verification of Inverse Square Law

1.4.1 Purpose

In this experiment we will verify the inverse square law, i.e. the count rate is inversely proportional to r^2, where r is the distance between detector and source.

1.4.2 Relevant Information

In explaining the inverse square law it is convenient to make the analogy between a light source and a gamma-ray source. Let us assume that we have a light source that emits light photons at a rate, n_0 photons/second. It is reasonable to assume that these photons are emitted in an isotopic manner, that is, equally in all directions.

If we place the light source in the center of a clear plastic spherical shell, it is quite easy to measure the number of light photons per second for each cm^2 of the spherical shell. This intensity is given by

$$I_0 = \frac{n_0}{4\pi d^2} \tag{1.7}$$

Where
n_0 is the total number of photons per second from the source,
d is the radius from the central source of light to the surface of the sphere.

Since n_0 is constant, I_0 is seen to vary as $\frac{1}{d^2}$. This is the inverse square law.

For a radioisotope, whose half-life is extremely long compared to the time taken to implement the series of measurements in this experiment, n_0 is synonymous with the activity, A_0, of

the radioactive source. Consequently, Equation 1.7 can be expressed as

$$R_0 = \frac{N}{T} = A_0 \frac{a_d}{4\pi d^2} \epsilon_{int} = \frac{C}{d^2} \tag{1.8}$$

Where
R_0 is the true counting rate derived from the GM tube,
N is the number of counts measured in the counting time T (corrected for dead time and background),
A_0 is the activity of the radioactive source,
ϵ_{int} is the intrinsic efficiency of the GM tube for detecting the gamma rays,
a_d is the effective sensitive area of the detector at its entrance window, and d is the distance from the point source to the entrance window of the detector and
$C = (A_0 a_d \epsilon_{int})/4\pi$ is a constant.

The factors in Equation 1.8 can be understood as follows. The effective sensitive area at the input to the detector intercepts a fraction,

$$\frac{a_d}{4\pi d^2},$$

of the total area of the sphere of radius d. Consequently, the detector intercepts that same fraction of the isotropic radiation emitted by the source. Only a fraction, ϵ_{int}, of the photons impinging on the sensitive area of the detector window are actually counted by the detector, due to window attenuation and the efficiency of converting photons into ionized atoms in the GM tube. The purpose of this experiment is to verify the $\frac{1}{d^2}$ dependence predicted by Equation 1.8.

In the measurement of the distance between the GM window and source, the top of the source holder may not coincide with the active surface of the source and, also the window of the GM tube may not coincide with the point where the ionisation actually takes place inside the detector. Hence, a correction factor has to be introduced.

Let $d = r + r_0$, where r is the measured distance and r_0 is the correction factor.

Replacing d in equation 1.8, we have

$$r = \sqrt{\frac{C}{R_0}} - r_0 \tag{1.9}$$

Thus, r_0 can be obtained from the intercept of r vs $\frac{1}{\sqrt{R_0}}$ plot. This correction factor r_0 has to be added to all values of r in further analysis.

1.4.3 Procedure

1. Set the GM tube at the proper operating voltage, and place a radioactive source 1 cm away from the face of the window or the closest slot available for source tray.

2. Count for a period of time long enough to get reasonable statistical precision ($\geq$ 4000 counts).

3. Move the source to 2 cm or next slot, and repeat the measurement for the same amount of time. Repeat the process with larger distances and tabulate the data in Table 1.4 (Note that for the longer distances the time will have to be increased to obtain the minimum number of counts necessary for adequate statistical precision)

Table 1.4: Data for verification of Inverse Square law

Distance (cm)	Count Rate N/T	Dead time corrected Counts	Background Counts	Corrected Counts (R_0)

4. Correct the counts, first for dead time and then for background, and fill in the corrected counting rate in Table 1.4.

5. On linear graph paper, plot the corrected counting rate (y axis) as a function of distance (x axis). This plot should have the $1/d^2$ characteristics exhibited by Equations 1.7 and 1.8. Typical plot of the data is shown in Fig. 1.13

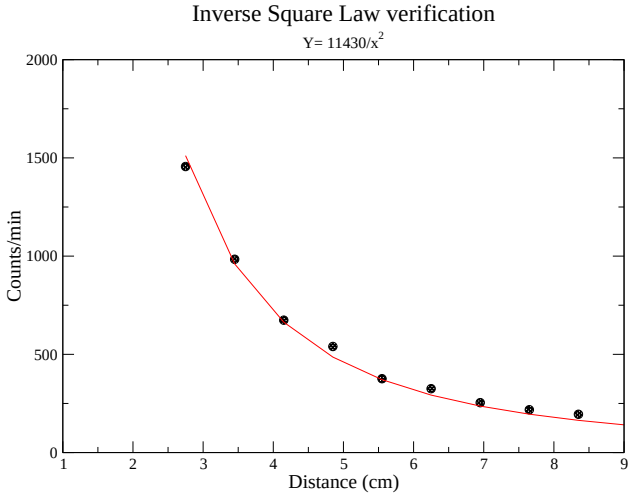

Figure 1.13: Variation of count rate with increasing distance. The data point are fitted with $y = const./x^2$

In the calculation of distance, d, the correction factor r_0 obtained from Fig. 1.14 has been included.

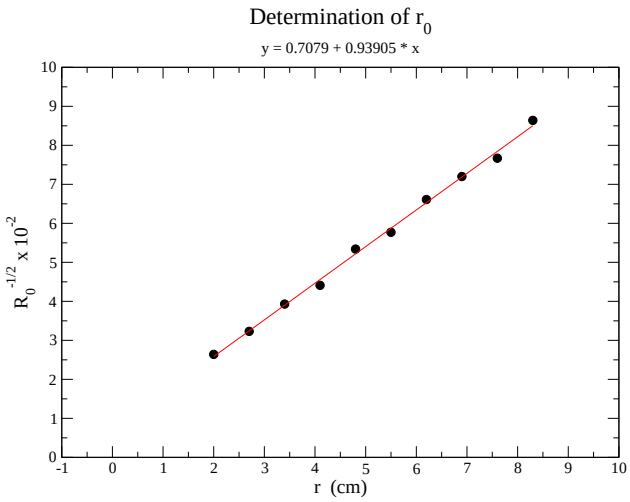

Figure 1.14: Plot for estimation of correction factor r_0

An alternative way to prove $1/d^2$ variation is to plot the data as log(R_0) vs log(d). The slope of the plot should be -2. A typical plot is shown in Fig. 1.15

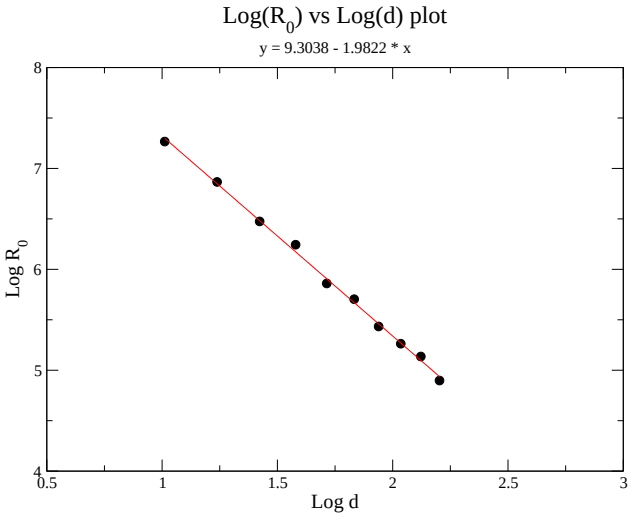

Figure 1.15: Plot of log(R_0) vs log(d). The data points are fitted with a linear function for which a slop of -1.98 is measured

1.4.4 Exercises

a. Calculate efficiency of the counter.

1.5 EXPERIMENT 4: Nuclear Counting Statistics

1.5.1 Purpose

The counting of nuclear radiations follows the Poisson and Gaussian distributions. In this experiment we will see how well these distributions apply to actual counting. A χ^2-test will be made to justify the goodness of fit.

1.5.2 Relevant information

Radioactive decay is a random process and each measurement made for a radioactive sample is independent of all previous measurements. Repeated individual measurements of the activity vary randomly. However, for a large number of repeated individual measurements, the deviation of the individual counts from the "average count" behaves in a predictable manner. Small deviations from the average are much more likely than large deviations. In this experiment, we will see that the frequency of occurrence of a particular deviation from this average, within a given size interval, can be determined with a certain degree of confidence. Nearly two hundred independent measurements will be made, and some rather simple statistical treatments of the data will be performed. The experiment utilizes a radioactive source which has a half-life that is very long compared to the measurement time. A half-life of few years ensures that the activity can be considered constant for the duration of the experiment.

The average count for n independent measurements is given by

$$N_{av} = \frac{N_1 + N_2 + N_3 + ... + N_n}{n} = \sum_{i=1}^{n} \frac{N_i}{n} \tag{1.10}$$

where N_1, N_2, N_3, ... N_n and N_i are the counts in the n independent measurements. The deviation of an individual count from the mean is (N_i - N_{av}). Based on the definition of N_{av}

$$\sum_{i=1}^{n} (N_i - N_{av}) = 0 \tag{1.11}$$

For cases where the percent dead time losses are small, it can be shown that the expected standard deviation, σ_N, can be estimated from

$$\sigma_N \simeq \sqrt{N_{av}} \simeq \sqrt{N_i} \tag{1.12}$$

with the estimate from N_{av} being more precise than the estimate from the individual measurement N_i. Thus, σ_N is the estimate of the standard deviation expected for the distribution of the measured counts, N_i, around the true mean.

Frequently, one is dealing with counting rates, rather than counts. If the true counting rate is defined by the number of counts accumulated in the counting time T, i.e.,

$$r_i = \frac{N_i}{T} \tag{1.13}$$

Then, the estimated standard deviation in the counting rate can be calculated from

$$\sigma_r = \frac{\sigma_N}{T} \simeq \frac{\sqrt{N_{av}}}{T} \simeq \frac{\sqrt{N_i}}{T} = \sqrt{\frac{r_i}{T}} \tag{1.14}$$

A meaningful way to express the statistical precision of the measurement is via the percent standard deviation, which is defined by

$$\sigma\% = \frac{\sigma_r}{r_i} \times 100\% = \frac{\sigma_N}{N_i} \times 100\% = \frac{100\%}{\sqrt{N_i}} \tag{1.15}$$

Note that achieving a 1% standard deviation requires 10,000 counts.

1.5.3 Procedure

1. Set the operating voltage of the Geiger tube at the value determined in Experiment 1.2.

2. Place the radioactive source in fourth/fifth slot from the window of the GM tube.

3. Without moving the source, take at least 200 or more independent 5 secs. runs and record the counts for each run in Table 1.5. The counter values, N_i, may be recorded directly in the table since, for this experiment, N_i is defined as the number of counts recorded for a 5 secs. time interval.

4. With a calculator determine N_{av}. You can also use excel sheet for further analysis. Fill in the values of $N_i - N_{av}$ in Table 1.5. It should be noted that these values can be either positive or negative. You should indicate the sign in the data entered in the table.

5. Calculate σ_N, and fill in the values for σ_N and $\frac{(N_i - N_{av})}{\sigma_N}$ in the table, using only two decimal places. Next, round off the values for $\frac{(N_i - N_{av})}{\sigma_N}$ to the nearest 0.5 and record the values in the "Rounded Off" column of the table.

6. Make a plot of the frequency of the rounded-off events $\frac{(N_i - N_{av})}{\sigma_N}$ vs. the rounded-off values. Fig. 1.16 shows this plot for an ideal case.

7. What kind of distribution does your plot follow?

Table 1.5: Data for the measurement of statistical distribution of radioactive decay

Run No.	Counts in 5 secs. (N_i)	σ_N	$N_i - N_{av}$	$\frac{N_i - N_{av}}{\sigma_N}$	$\frac{N_i - N_{av}}{\sigma_N}$ Rounded off

Table 1.6: Frequency distribution of a measured data readings

Bins	-2.5	-2.0	-1.5	-1.0	-0.5	0	0.5	1.0	1.5	2.0	2.5
No. of readings (O_k)		1	3	17	18	24	18	11	7	1	

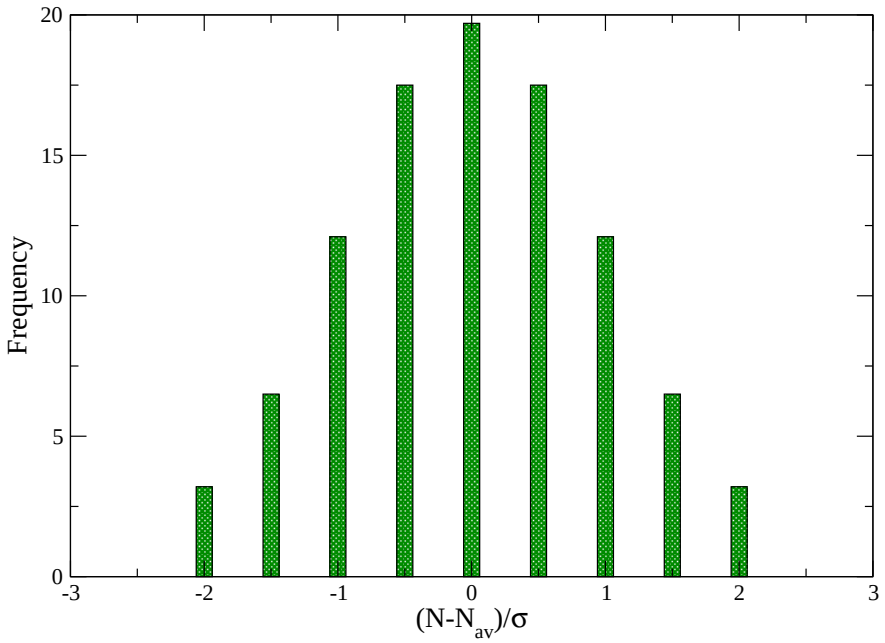

Figure 1.16: Gaussian distribution function.

1.5.4 Exercises

a. Repeat the steps 1-7 without a radioactive source, i.e. find out the distribution plot for background radiation. Note that in this case counts

measured by the detector may be less than 10. Comment on the difference between the two plots.

b. Which distribution matches the data with the background counts? How well does the Gaussian distribution describe the source data?

c. How close are the standard deviation values when calculated with the Poisson and Gaussian distributions?

A typical plot for statistical distribution measured with GM counter is shown in Fig. 1.17.

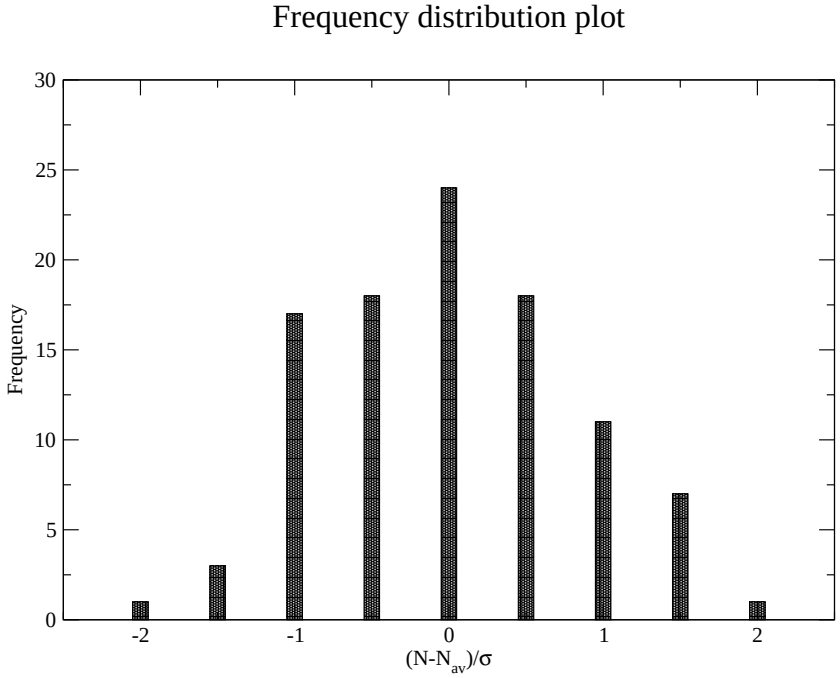

Figure 1.17: Illustration of statistical distribution of radioactive decay process measured using GM detector.

1.5.5 χ^2-test of the statistical data

In the above experiment, counting of nuclear radiation was repeated 200 times keeping the time interval fixed. The best value of the count were obtained by taking mean of all the counts

$$N_{av} = \frac{1}{n} \sum N_i, \tag{1.16}$$

where n is total number of observations and N_i are the counts. The standard deviation σ were calculated as

$$\sigma = \sqrt{\frac{\sum (N_i - N_{av})}{n-1}} \tag{1.17}$$

The factor $(n-1)$ in the denominator is due to finite number of readings. Using the observed counts a frequency distribution of the data were produced. This can be compared with expected number of events using a Gaussian or Poisson distribution. If the difference between the observed number O_k for a bin k and the corresponding expected number E_k is small we can say that the Gaussian or Poisson distribution is a good assumption for the data points. The E_k can be calculated for Gaussian distribution function using the Table 1.20 given in the Appendix of this chapter.

The χ^2-test is meant to find out the goodness of fit. χ^2 is defined in our case as :

$$\chi^2 = \sum_{k=1}^{n} \frac{(O_k - E_k)^2}{E_k} \tag{1.18}$$

If $\chi^2 = 0$, the agreement is perfect, i.e. $O_k = E_k$ for all the bins k. This situation is very unlikely to occur. In general, the individual terms in the sum is of the order of one and since there are n terms in the sum,

$$\chi^2 \leq n$$

can be considered as a good agreement. On the other hand, if

$$\chi^2 >> n,$$

we can say that there is significant disagreement between the observed data and the expected distribution function.

Degrees of freedom

The degrees of freedom f in a statistical calculation is defined as the number of observed data minus the number of parameters computed from the data and used in the calculation. If the observed data O_k are distributed in k bins and c is the number of parameters that had to be calculated from the data to compute E_k, then the degrees of freedom is given by

$$f = k - c \tag{1.19}$$

The number of constraints c depends upon specific example under consideration. In the above example of radioactivity measurement, total number of readings N=200 was distributed among 9 bins, as shown in Table 1.6. It is clear that total number of readings follows equation 1.20. This means that if we know values of O_k in eight bins, the last one can be calculated using the relation 1.20. Therefore, the equation 1.20 represents one of the constraints.

$$N = \sum_k O_k \tag{1.20}$$

We need to know mean μ and variance σ for estimation of number of readings, E_k, following Gaussian distribution function. We have seen that these parameters were obtained using the 200 data readings. Therefore, in this example, total number of constraints are three and degrees of freedom f can be calculated as 9-3=6.

Reduced χ^2 and goodness of fit

The reduced χ^2 is defined as

$$\bar{\chi}^2 = \frac{\chi^2}{F} = \frac{1}{F}\sum_{k=1}^{n}\frac{(O_k - E_k)^2}{E_k} \tag{1.21}$$

Note that the reduced $\bar{\chi}^2$ should be of the order of 1. If $\bar{\chi}^2 >> 1$, the data do not fit the assumed distribution satisfactorily.

We will analyse the data taken in the previous section. The calculated number of readings following Gaussian distribution are compared with the observed readings in Table 1.7. A χ^2 value of 8.03 has been calculated using the data given in Table 1.7. Since degrees of freedom in this case is six, the reduced $\bar{\chi}^2$ value is 1.34.

Table 1.7: Observed and calculated frequency distribution for radioactive decay measurement

Bins	-2.5	-2.0	-1.5	-1.0	-0.5	0	0.5	1.0	1.5	2.0	2.5
No. of readings (O_k)		1	3	17	18	24	18	11	7	1	
Gaussian Dist. (E_k)		3.2	6.6	12.1	17.5	19.7	17.5	12.1	6.6	3.2	

Now one can ask if the value of $\bar{\chi}^2$=1.34 is sufficiently larger than one to rule out our expected Gaussian distribution. Standard tables are available (see Table 1.21 in Appendix of this chapter) for percentage probability $Prob_f(\bar{\chi}^2 \geq \bar{\chi_0}^2)$ of obtaining the value of $\bar{\chi}^2$ greater than or equal to any particular value $\bar{\chi_0}^2$, assuming the measurements concerned are governed by the expected distribution.

The table shows that probability for obtaining $\bar{\chi}^2 \geq 1.34$ with six degree of freedom is 25% which is OK. Any value less than 5 suggest that our data is not consistent with the expected distribution function.

1.6 APPENDIX: Statistical Distribution Function

1.6.1 Binomial distributions:

The binomial distribution is the most general of the statistical models and is widely applicable to all constant probability processes. If n is the number of trials for which each trial has a success probability p, then the predicted probability of counting exactly x successes is given by

$$P(x) = \frac{n!}{(n-x)!x!} p^x (1-p)^{n-x} \tag{1.22}$$

$P(x)$ is the predicted probability distribution function, as given by the binomial distribution, and is defined only for integer values of n and x. The Binomial distribution function is shown in Fig. 1.18.

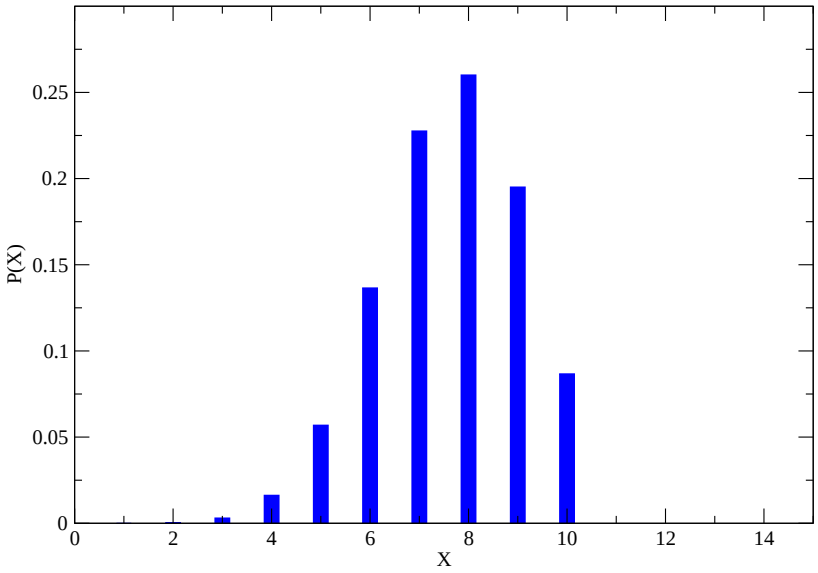

Figure 1.18: Binomial distribution function.

Properties of binomial distributions:

$$\sum_{x=0}^{n} P(x) = 1 \tag{1.23}$$

$$\bar{x} = \sum_{x=0}^{n} xP(x) \tag{1.24}$$

substituting the value of $P(x)$ we have

$$\bar{x} = pn \tag{1.25}$$

It is also important to derive a single parameter that can be describe the amount of fluctuation predicted by a given distribution. We can define a predicted variance σ^2, which is a measure of the scatter about the mean predicted by a specific statistical model $P(x)$:

$$\sigma^2 = \sum_{x=0}^{n} (x - \bar{x})^2 P(x) \tag{1.26}$$

Putting the value of $P(x)$ we have $\sigma^2 = np(1-p)$.

1.6.2 Poisson Distribution

Many categories of binary processes can be characterized by a constant and small probability of success for each individual trials. Included are most nuclear counting experiments in which the number of nuclei are large and measuring time is small compared to half-life of the radioactive species. Under these condition, the approximation holds that the success probability is small and constant and the binomial distribution reduces to the Poisson form.

Let us take the binomial distribution for p $<<$ 1. We are interested in its behavior as n becomes infinitely large while the mean μ =np remains constant. We can write the binomial distribution as

$$P(x) = \frac{n!}{x!(n-x)!} p^x (1-p)^{-x} (1-p)^n \tag{1.27}$$

we can write

$$\frac{n!}{(n-x)!} = n(n-1)(n-2)....(n-x+2)(n-x+1) \tag{1.28}$$

and in the limit $x << n$ each factor is equal to n and this term asymptotically approaches n^x . The term $(1-p)^{-x}$ is approximately $(1+px)$ which asymptotically approaches 1 as p becomes infinitesimally small. The last term can be rearranged by substituting μ/p for n to show that it asymptotically approaches $e^{-\mu}$

Combining these approximations, we find that the binomial distribution probability function $P(x)$ asymptotically approaches the Poisson distribution

$$P(x, \mu) = \frac{\mu^x}{x!} \, \mathrm{e}^{-\mu} \tag{1.29}$$

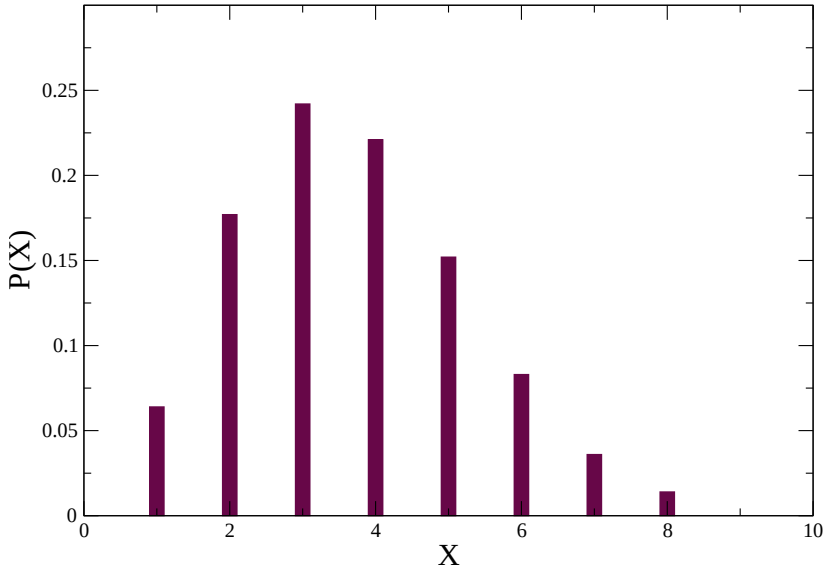

Figure 1.19: Poisson distribution function.

We note that significant simplification has occurred in deriving the Poisson distribution - only one parameter is required, which is the mean μ. This is a great help for processes in which we can in some way measure or estimate the mean value, but for which we have no idea of either the individual probability or the size of the sample. Such is usually the case in nuclear measurement.

In order to verify the normalization of the distribution function is correct we note that the first term i.e.

$$\sum_{x=0}^{\infty} \frac{\mu^x}{x!} = \mathrm{e}^{\mu} \tag{1.30}$$

Mean and standard deviation

The mean μ of the Poisson distribution must be the same parameter μ which appear in the probability distribution function because that is the mean of the corresponding binomial distribution.

$$< x >= \sum_{x=0}^{\infty} x \frac{\mu^x}{x!} \mathrm{e}^{-\mu} = \mu \mathrm{e}^{-\mu} \sum_{x=1}^{\infty} \frac{\mu^{x-1}}{(x-1)!} = \mu \mathrm{e}^{-\mu} \sum_{y=0}^{\infty} \frac{\mu^y}{y!} = \mu \tag{1.31}$$

The variance σ^2 can be evaluated by examining behavior of binomial distribution in the limit that p becomes infinitesimally small.

$$\sigma^2 = \lim_{p \to 0} [np(1-p)] = \mu \tag{1.32}$$

Alternatively, the expectation value of the square of the deviation can be evaluated directly

$$\sigma^2 =< (x-\mu)^2 >= \sum_{x=0}^{\infty} [(x-\mu)^2 \frac{\mu^x}{x!} \mathrm{e}^{-\mu}] = \mu \tag{1.33}$$

The standard deviation σ is therefore square root of the the mean μ.

1.6.3 Gaussian Distribution

The most important probability distribution for use in the statistical analysis of data is the Gaussian or normal distribution. Mathematically, it is an approximation to the binomial distribution for the special limiting case where the number of observation n is infinitely large and the probability of success for each is finitely large so that $np >> 1$.

The Gaussian distribution is a continuous symmetric distribution function of the form $exp\,[-x^2/2\sigma^2]$. The function has the value 1 at x=0 and it decreases symmetrically as the value of x changes from the value zero. Gaussian function representing a symmetric function around the mean value μ is given by $exp\,[-(x-\mu)^2/2\sigma^2]$

The sharpness of the function, i.e. how fast function goes to zero as x changes from its mean value depends upon the parameter σ. if the value of σ is small the exponent $x^2/2\sigma^2$ will be large resulting the function to decrease steeper.

Now any probability function must satisfy the condition

$$\int_{-\infty}^{+\infty} N\ exp\left[-(x-\mu)^2/2\sigma^2\right] dx = 1 \tag{1.34}$$

The normalising factor N can be evaluated as $\frac{1}{\sigma\sqrt{2\pi}}$.

The Gaussian function is therefore represented by

$$P(x) = \frac{1}{\sigma\sqrt{2\pi}} \exp[\frac{-(x-\mu)^2}{2\sigma^2}] \tag{1.35}$$

The two parameters μ and σ^2 correspond to the mean and variance of the distribution. This we can verify using their basic definition.

Mean

$$\bar{x} = \int_{-\infty}^{+\infty} x \frac{1}{\sigma\sqrt{2\pi}} exp\left[-(x-\mu)^2/2\sigma^2\right] dx \tag{1.36}$$

Let us define $z = x - \mu$, such that $dz = dx$ and $x = z + \mu$

replacing the variables, we have

$$\bar{x} = \frac{1}{\sigma\sqrt{2\pi}} \left(\int_{-\infty}^{+\infty} z \; exp\left[-z^2/2\sigma^2\right] dz + \mu \int_{-\infty}^{+\infty} exp\left[-z^2/2\sigma^2\right] dz \right) \tag{1.37}$$

The first integral is zero as it is an odd integral and the second integral is $\sigma\sqrt{2\pi}$. Therefore, we have $\bar{x} = \mu$.

Standard deviation

Using the definition of standard deviation we can write

$$\sigma_x^2 = \int_{-\infty}^{+\infty} (x-\mu)^2 \frac{1}{\sigma\sqrt{2\pi}} exp\left[-(x-\mu)^2/2\sigma^2\right] dx \tag{1.38}$$

replacing the variable once again by $z = x - \mu$ and evaluating the integral by parts, we have $\sigma_x^2 = \sigma^2$

Significance of Standard deviation

The area under the probability distribution curve represent the total probability of the event to occur. If the event is described by the Gaussian distribution and now we ask what is the probability of obtaining the value x between $\mu \pm \sigma$. We can calculate this by evaluating the integral

$$P_{1\sigma} = \frac{1}{\sigma\sqrt{2\pi}} \left(\int_{\mu-\sigma}^{\mu+\sigma} exp\left[-(x-\mu)^2/2\sigma^2\right] dx \right) \tag{1.39}$$

substituting the $(x-\mu)/\sigma = z$ such that $dx = \sigma \; dz$ and the limits of the new variable z will be ± 1

we can write the integral as

$$P_{1\sigma} = \frac{1}{\sqrt{2\pi}} \left(\int_{-1}^{1} exp\left(-z^2/2\right) dz \right) \tag{1.40}$$

The above integral is called as "error integral" and its value can be computed as 0.68. That means the probability of finding the value of x with one σ limit is 68%. Similarly, probability of finding the value of x within 2σ and 3σ limits are 95.4% and 99.7%, respectively. A table for the error integral is given in the following.

Sometime the width of the distribution function is described by the quantity Γ called as "Full Width at Half Maximum" (FWHM).

This is defined as the range of x between the values at which the probability $P(x, \mu, \sigma)$ is half its maximum value.

$$P(\mu \pm \frac{1}{2}\Gamma, \mu, \sigma) \; = \frac{1}{2} P(\mu, \mu, \sigma) \tag{1.41}$$

which gives $\Gamma = 2.354\sigma$

Appendix B: Normal Error Integral, II

Table B. The percentage probability, $Q(t) = \int_X^{X+t\sigma} G_{X,\sigma}(x)\,dx$, as a function of t.

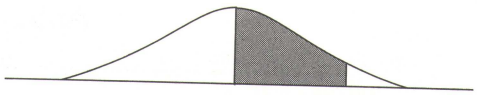

t	0.00	0.01	0.02	0.03	0.04	0.05	0.06	0.07	0.08	0.09
0.0	0.00	0.40	0.80	1.20	1.60	1.99	2.39	2.79	3.19	3.59
0.1	3.98	4.38	4.78	5.17	5.57	5.96	6.36	6.75	7.14	7.53
0.2	7.93	8.32	8.71	9.10	9.48	9.87	10.26	10.64	11.03	11.41
0.3	11.79	12.17	12.55	12.93	13.31	13.68	14.06	14.43	14.80	15.17
0.4	15.54	15.91	16.28	16.64	17.00	17.36	17.72	18.08	18.44	18.79
0.5	19.15	19.50	19.85	20.19	20.54	20.88	21.23	21.57	21.90	22.24
0.6	22.57	22.91	23.24	23.57	23.89	24.22	24.54	24.86	25.17	25.49
0.7	25.80	26.11	26.42	26.73	27.04	27.34	27.64	27.94	28.23	28.52
0.8	28.81	29.10	29.39	29.67	29.95	30.23	30.51	30.78	31.06	31.33
0.9	31.59	31.86	32.12	32.38	32.64	32.89	33.15	33.40	33.65	33.89
1.0	34.13	34.38	34.61	34.85	35.08	35.31	35.54	35.77	35.99	36.21
1.1	36.43	36.65	36.86	37.08	37.29	37.49	37.70	37.90	38.10	38.30
1.2	38.49	38.69	38.88	39.07	39.25	39.44	39.62	39.80	39.97	40.15
1.3	40.32	40.49	40.66	40.82	40.99	41.15	41.31	41.47	41.62	41.77
1.4	41.92	42.07	42.22	42.36	42.51	42.65	42.79	42.92	43.06	43.19
1.5	43.32	43.45	43.57	43.70	43.82	43.94	44.06	44.18	44.29	44.41
1.6	44.52	44.63	44.74	44.84	44.95	45.05	45.15	45.25	45.35	45.45
1.7	45.54	45.64	45.73	45.82	45.91	45.99	46.08	46.16	46.25	46.33
1.8	46.41	46.49	46.56	46.64	46.71	46.78	46.86	46.93	46.99	47.06
1.9	47.13	47.19	47.26	47.32	47.38	47.44	47.50	47.56	47.61	47.67
2.0	47.72	47.78	47.83	47.88	47.93	47.98	48.03	48.08	48.12	48.17
2.1	48.21	48.26	48.30	48.34	48.38	48.42	48.46	48.50	48.54	48.57
2.2	48.61	48.64	48.68	48.71	48.75	48.78	48.81	48.84	48.87	48.90
2.3	48.93	48.96	49.98	49.01	49.04	49.06	49.09	49.11	49.13	49.16
2.4	49.18	49.20	49.22	49.25	49.27	49.29	49.31	49.32	49.34	49.36
2.5	49.38	49.40	49.41	49.43	49.45	49.46	49.48	49.49	49.51	49.52
2.6	49.53	49.55	49.56	49.57	49.59	49.60	49.61	49.62	49.63	49.64
2.7	49.65	49.66	49.67	49.68	49.69	49.70	49.71	49.72	49.73	49.74
2.8	49.74	49.75	49.76	49.77	49.77	49.78	49.79	49.79	49.80	49.81
2.9	49.81	49.82	49.82	49.83	49.84	49.84	49.85	49.85	49.86	49.86
3.0	49.87									
3.5	49.98									
4.0	49.997									
4.5	49.9997									
5.0	49.99997									

Figure 1.20: Table for Normal error integral.

Appendix D: Probabilities for Chi Squared

Table D. The percentage probability $Prob_d(\tilde{\chi}^2 \geq \tilde{\chi}_o^2)$ of obtaining a value of $\tilde{\chi}^2 \geq \tilde{\chi}_o^2$ in an experiment with d degrees of freedom, as a function of d and $\tilde{\chi}_o^2$. (Blanks indicate probabilities less than 0.05%.)

	$\tilde{\chi}_o^2$															
d	0	0.5	1.0	1.5	2.0	2.5	3.0	3.5	4.0	4.5	5.0	5.5	6.0	8.0	10.0	
1	100	48	32	22	16	11	8.3	6.1	4.6	3.4	2.5	1.9	1.4	0.5	0.2	
2	100	61	37	22	14	8.2	5.0	3.0	1.8	1.1	0.7	0.4	0.2			
3	100	68	39	21	11	5.8	2.9	1.5	0.7	0.4	0.2	0.1				
4	100	74	41	20	9.2	4.0	1.7	0.7	0.3	0.1	0.1					
5	100	78	42	19	7.5	2.9	1.0	0.4	0.1							
	0	0.2	0.4	0.6	0.8	1.0	1.2	1.4	1.6	1.8	2.0	2.2	2.4	2.6	2.8	3.0
1	100	65	53	44	37	32	27	24	21	18	16	14	12	11	9.4	8.3
2	100	82	67	55	45	37	30	25	20	17	14	11	9.1	7.4	6.1	5.0
3	100	90	75	61	49	39	31	24	19	14	11	8.6	6.6	5.0	3.8	2.9
4	100	94	81	66	52	41	31	23	17	13	9.2	6.6	4.8	3.4	2.4	1.7
5	100	96	85	70	55	42	31	22	16	11	7.5	5.1	3.5	2.3	1.6	1.0
6	100	98	88	73	57	42	30	21	14	9.5	6.2	4.0	2.5	1.6	1.0	0.6
7	100	99	90	76	59	43	30	20	13	8.2	5.1	3.1	1.9	1.1	0.7	0.4
8	100	99	92	78	60	43	29	19	12	7.2	4.2	2.4	1.4	0.8	0.4	0.2
9	100	99	94	80	62	44	29	18	11	6.3	3.5	1.9	1.0	0.5	0.3	0.1
10	100	100	95	82	63	44	29	17	10	5.5	2.9	1.5	0.8	0.4	0.2	0.1
11	100	100	96	83	64	44	28	16	9.1	4.8	2.4	1.2	0.6	0.3	0.1	0.1
12	100	100	96	84	65	45	28	16	8.4	4.2	2.0	0.9	0.4	0.2	0.1	
13	100	100	97	86	66	45	27	15	7.7	3.7	1.7	0.7	0.3	0.1	0.1	
14	100	100	98	87	67	45	27	14	7.1	3.3	1.4	0.6	0.2	0.1		
15	100	100	98	88	68	45	26	14	6.5	2.9	1.2	0.5	0.2	0.1		
16	100	100	98	89	69	45	26	13	6.0	2.5	1.0	0.4	0.1			
17	100	100	99	90	70	45	25	12	5.5	2.2	0.8	0.3	0.1			
18	100	100	99	90	70	46	25	12	5.1	2.0	0.7	0.2	0.1			
19	100	100	99	91	71	46	25	11	4.7	1.7	0.6	0.2	0.1			
20	100	100	99	92	72	46	24	11	4.3	1.5	0.5	0.1				
22	100	100	99	93	73	46	23	10	3.7	1.2	0.4	0.1				
24	100	100	100	94	74	46	23	9.2	3.2	0.9	0.3	0.1				
26	100	100	100	95	75	46	22	8.5	2.7	0.7	0.2					
28	100	100	100	95	76	46	21	7.8	2.3	0.6	0.1					
30	100	100	100	96	77	47	21	7.2	2.0	0.5	0.1					

The values in Table D were calculated from the integral

$$Prob_d(\tilde{\chi}^2 \geq \tilde{\chi}_o^2) = \frac{2}{2^{d/2}\Gamma(d/2)} \int_{\chi_o}^{\infty} x^{d-1} e^{-x^2/2} dx.$$

See, for example, E. M. Pugh and G. H. Winslow, *The Analysis of Physical Measurements* (Addison-Wesley, 1966), Section 12-5.

Figure 1.21: The percentage probabilities for Chi squared.

1.7 EXPERIMENT 5 : Absorption coefficient for γ rays passing through Lead, Copper and Aluminium absorbers.

1.7.1 Purpose

1. To determine linear absorption coefficient, μ, for γ rays passing through Lead, Copper and Aluminium absorbers.

2. Variation of μ with atomic number Z.

1.7.2 Relevant information

Gamma-rays lose energy while passing through matter by three main processes, viz., photo-electric absorption, Compton scattering and pair-production. The intensity of the radiation is thus decreased as a function of distance in the absorbing medium. The purpose of this experiment is to measure the attenuation of the intensity with absorber thickness, and to derive the half-thickness and the attenuation coefficient. When a γ-ray flux of intensity I_0 passes through a substance of thickness x, the outgoing intensity I is given by

$$I = I_0 e^{-\mu x} \tag{1.42}$$

where μ is the linear absorption coefficient for γ-ray, the value of which depends on the material (atomic numbers of the elements and their relative weights constituting the material) and the energy of the incident γ-ray. The μ in the above expression is the sum of photoelectric μ_p and Compton scattering μ_c absorption coefficients:

$$\mu = \mu_p + \mu_c \tag{1.43}$$

It is convenient to express the thickness x as ρx where ρ is the density of the material under study. The unit of thickness for this way of expressing it is grams/cm^2 .

Then

$$I = I_0 e^{(-\mu/\rho)\rho x} \tag{1.44}$$

Accordingly μ/ρ is now called mass absorption coefficient and is expressed in cm^2/gm.

Following are the advantages of choosing this unit:

(i) Measurement of the thickness of a very thin foil is often quite inconvenient. On the other hand its area and weight can be measured easily and accurately from which its thickness in gm/cm^2 can be obtained.

(ii) The energy loss due to ionisation per unit distance of travel of an incident β-particle is proportional to the number of atomic electrons/cm^3 ($= NZ$) in the absorber material. Here, N is the number of atoms/cm^3 and Z is the atomic number of the element. We can also write

$$NZ = (\frac{\rho N_A}{A})Z = \rho N_A \frac{Z}{A} \tag{1.45}$$

where N_A is the Avogadro number and ρ is the density in gm/cm^3 of the absorber material. Interestingly, (Z/A) is nearly constant for all elements and thus the ionisation loss (in ergs gm^{-1}cm^{-2}) becomes approximately independent of the choice of the material making the absorber. The above considerations apply equally well to absorbers made from alloys and compounds.

The half-value thickness $x_{1/2}$ is defined as the thickness of the absorber for which the γ-ray intensity gets reduced to half of the incident intensity (corresponding to $x = 0$). The following relationship is useful :

$$x_{1/2} = \frac{0.693}{\mu} \tag{1.46}$$

We will find the value of μ for any given material at a few γ-ray energies.

1.7.3 Procedure

The experimental arrangement is shown in Fig. 1.22. Make the GM setup in operation, as discussed in previous experiments.

A lead collimator can be used to collimate the γ-rays from the source towards the absorber. This will minimize scattering from the surrounding objects which would otherwise have reached the detector to unduly contribute to the true counts. However, we do not have collimeters for this experiment.

1. Set the voltage of the Geiger tube at the operating value determined in the first experiment.

2. Place a radioactive source about 4 cm from the window of the Geiger tube, and count for 2 minutes. Record the number of counts (I_0).

3. First, we will use the lead absorbers. The thickness of the absorbers can be measured using a screw gauge. Suitable combination of the absorbers will be used to increment the total thickness.

Figure 1.22: Experimental arrangement for γ-ray absorption measurement.

4. Place the thinnest sheet of lead from the absorber kit between the source and the GM tube window and take another 2-minute count (I). Record the value.

5. Add a second sheet of lead on top of the first to increase the total thickness, and record the count.

6. Continue inserting combinations of lead sheets to increment the total thickness until the number of counts is 10% of the number recorded with no absorber (I_0). Record the counts taken in 2 minutes for each step.

1.7.4 Exercises

a. Correct all the measured counting rates for the dead time measured in previous experiment, if the correction alters the result by more than 1%. This correction should be applied before the background is subtracted.

7. Remove the source to a long distance from the counting station and make a 2-minute background run, and subtract this value from each of the above counts that have been corrected for dead time. Check this background count at the maximum absorber thickness employed and without any absorbers. The result should be the same, or close enough to the same that the average of the two background readings can be used for background subtraction from all the corrected counting rates with the source in the counting position.

8. Repeat the processes (1-8) for Al and Cu absorbers.

1.7.5 Exercises

b. Record the total density-thickness of the absorbers in mg/cm^2 and plot on semilog paper the corrected counts as a function of absorber density-thickness in mg/cm^2. The density-thickness is defined as the product of density in mg/cm^3 times the thickness of the absorber in cm.

c. Draw the best straight line through the points, and determine $x_{1/2}$ and μ from the slope of the line. Compare the results with the standard values

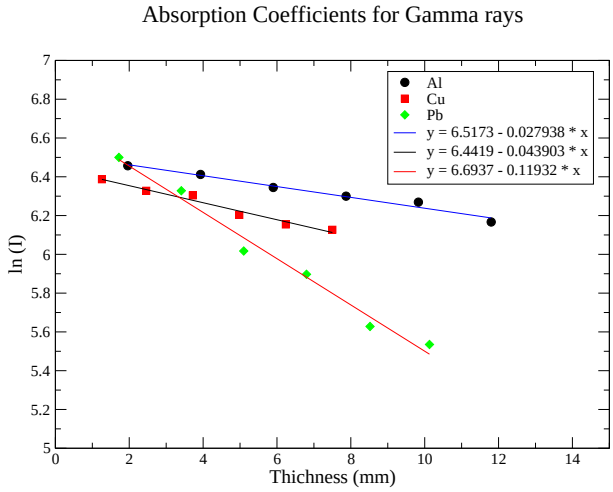

Figure 1.23: The plot of ln(I) vs absorber thickness for Al, Cu and Pb materials. The data points are fitted with a straight line for which the slop determines the absorption coefficient.

Typical plots for Al, Cu and Pb absorbers are show in Fig. 1.23. The linear absorption coefficient were obtained from the slope of the plot of Fig. 1.23. The measured half-value thickness and the standard values of linear absorption coefficient (μ) for different materials are listed in Table 1.8

Table 1.8: Linear absorption coefficient and half-value thickness measured for different materials. Standard values are also shown.

Material	Measured μ (mm^{-1})	Standard μ (mm^{-1})	$x_{1/2}$ (mm)
Aluminium (Al) Density= 2.70 gm/cm^3	0.028	0.021	24.8
Copper (Cu) Density= 8.92 gm/cm^3	0.044	0.068	15.8
Lead (Pb) Density= 11.34 gm/cm^3	0.119	0.142	5.8

1.8 EXPERIMENT 6 : Absorption curve for β-particles in Aluminum and determination of the end-point energy from range-energy relation.

1.8.1 Purpose

1. To determine range of β particles in Al.

2. Determination of end-point energy using Range-Energy relation.

1.8.2 Relevant information

As a β^--particle (electron) travels in an absorbing medium, it loses energy. As a result, it gradually slows down till it comes to rest. In other words, it is finally absorbed. An electron having an incident kinetic energy of 1 MeV suffers more than 10^4 collisions in an absorber before being stopped.

An electron gives away its energy through various interactions with the atoms and nuclei constituting the absorber. The most predominant one is coulomb interaction. The radiative process, although of somewhat less significance, is also a cause of energy loss by fast electrons in matter.

In our experiment, we are concerned with β^--particles which have a distribution in energy. The end-point energy E_β^{max} of 2 MeV is about the highest energy we have to deal with in the laboratory.

Ionisation and excitation are the most important outcome of coulomb interaction between β^--particles and atomic electrons. The ejected electron and the optical radiation emitted on excitation are also absorbed within a short distance in the same material. In effect, an incident β^-- particle finally loses its entire energy and is absorbed.

The specific energy loss (loss of energy per unit path length) due to collision inducing ionisation and excitation of the atoms by fast electrons (β^--particles emitted from our laboratory sources are fast electrons) is given by Bethe-Bloch equation:

$$-\left(\frac{dE}{dX}\right)_c = \frac{2\pi e^4 NZ}{m_0 v^2}\left[ln\frac{m_0 v^2 E}{2I^2(1-\beta^2)} - ln\ 2\left(2\sqrt{1-\beta^2} - 1 + \beta^2\right) + \left(1-\beta^2\right) + \frac{1}{8}\left(1-\sqrt{1-\beta^2}\right)^2\right],$$

where e = electronic charge, $\beta = v/c$, N = number of atoms per cm^3 in the absorber, Z = atomic number of the element constituting the absorber, m_0 = electron mass, c = velocity of light in vacuum, E = kinetic energy of the incident electron and I = average

ionisation/excitation potential of the atoms in the absorber.

In addition to the loss due to ionisation and excitation, radiative process is also a cause of energy loss by electrons while traveling in matter. As an energetic electron moves past a nucleus of an atom of the absorber it gets accelerated. As a result, electromagnetic radiation in the form of γ-rays are emitted. This is known as bremsstrahlung. The corresponding specific energy loss is :

$$-\left(\frac{dE}{dX}\right)_r = \frac{NEZ(Z+1)e^4}{137m_0^2c^4}\left(4\ ln\frac{2E}{m_0c^2} - \frac{4}{3}\right) \tag{1.47}$$

We see from this equation that radiative energy loss is higher for higher incident electron energies and higher Z of the absorber atoms. The loss will be less for heavy charged particles due to presence of the m_0^2 factor in the denominator of the multiplicative term of equation 1.47. The total specific energy loss is the sum of the above two energy losses. It is interesting to find the relative contribution of these two processes. The ratio of them is approximately :

$$\frac{(dE/dX)_r}{(dE/dX)_c} \simeq \frac{EZ}{700}, \tag{1.48}$$

where E is in MeV. Taking average electron energy to be 1 MeV in our experiments, we can calculate the ratio as given in the following Table 1.9: The ratios clearly show that energy loss through bremsstrahlung is quite small compared to that due to ionisation and excitation.

Table 1.9: The ratio between radiative and non-radiative process for different materials for 1 MeV β particles

Element	Z	$[(dE/dX)_r]$ / $[(dE/dX)_c]$
Aluminium	13	0.019
Copper	29	0.04
Silver	47	0.067
Lead	82	0.117

Absorption curves for β^- particles in Al are shown in Fig. 1.24. Range of an electron in an absorber is the distance it travels in it from the point of incidence to the point where it stops. The actual path followed by the electron is, however, not straight but somewhat zigzag. Range is therefore an effective path length considered straight.

Since the β^- particles have an energy distribution, the range R corresponds to that of the β^- particles having energy $E_\beta{}^{max}$. Range-energy relations established to find $E_\beta{}^{max}$ take care of all the β^--particles having a distribution in energy. The range energy relations of our interest are given below. These relations are linear for $E_\beta{}^{max} > 0.8$ MeV. Here, R is expressed in gm/cm^2 and $E_\beta{}^{max}$ in MeV.

Glendenin's relation :

$$R = 0.542E_\beta^{max} - 0.133 \tag{1.49}$$

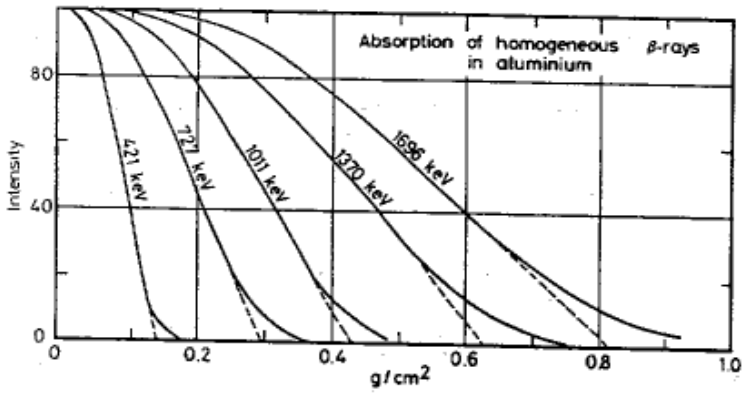

Figure 1.24: Absorption of β^-−particles in Aluminum. Range of beta particle can be determined by extrapolating the curve to the background count level.

Bleuler and Zunti's relation :

$$R = 0.571 E_\beta^{max} - 0.161 \tag{1.50}$$

A typical range-energy relationship for beta particles obtained from empirical relations is shown in Fig. 1.25.

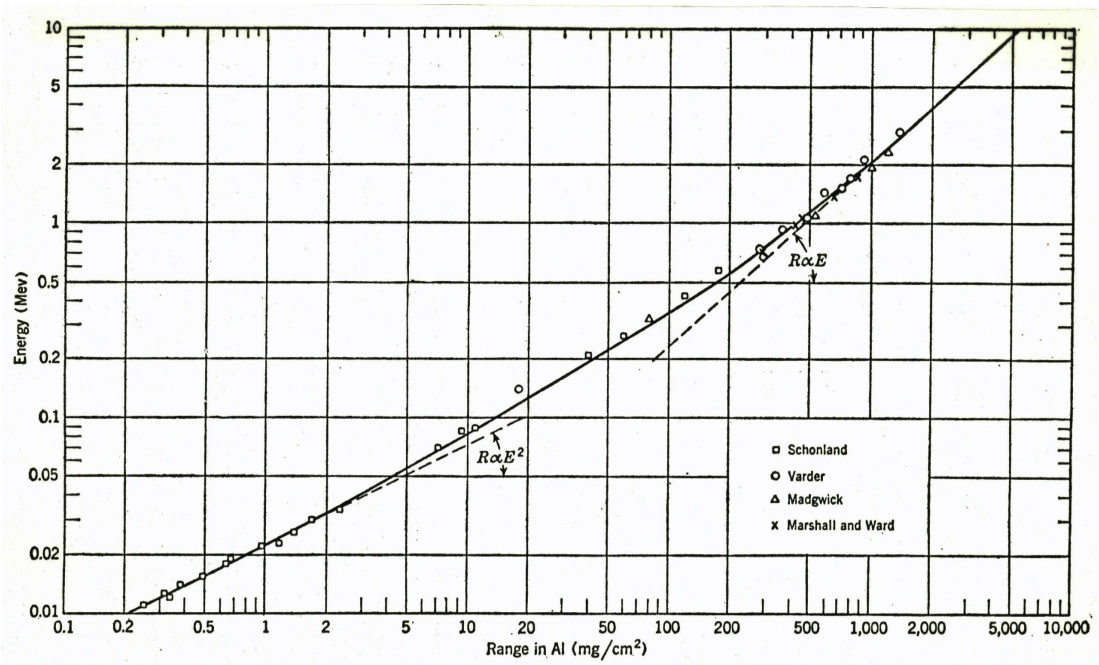

Fig. 3.3 Empirical range-energy relationship for electrons absorbed in aluminum. Experimental values by several observers (S16, V4, M4, M17) on monoenergetic electrons are shown. For *monoenergetic electrons*, the range coordinate refers to the *extrapolated range* R_0 of Fig. 3.2. For *continuous β-ray spectra* the energy coordinate refers to the end-point energy E_{max}, and the range coordinate becomes the *maximum range* R_m of Fig. 3.4. The smooth curve represents the empirical relationship, Eqs. (3.3) and (3.4), developed by Katz and Penfold (K7).

Figure 1.25: Range-Energy plot obtained from empirical relations for beta particles in Al absorber.

Our aim of the experiment is to find out the range of β^- -particles in aluminum and to determine $E_\beta{}^{max}$ from the range energy relation. One way to determine end-point energy, E_β^{max}, of the β particles is through Fermi-Kurie plot of their energy distribution data obtained from a magnetic beta spectrometer. This experiment was performed in previous semester. In the absence of such spectrometer the absorption experiment provides an alternative way to determine E_β^{max}. Besides, the effects arising from absorption of β^--radiation in biological systems and the consequent medical implications also add to the importance of an absorption experiment.

1.8.3 Procedure

The G. M. Counter setup to be used in this experiment is the same as the one used in previous experiments (see Fig. 1.22).

1. Start the G.M. counter setup.

2. Record the background counts for 5 min.

3. Place a ^{204}Tl β^- source on the source tray and put the tray into a slot of the stand about 5-6 cm away from the face of the counter. Do not disturb the source during data acquisition. This will change the count which is not because of absorption.

4. Take a blank absorber ring. Place it on the absorber tray; then put it is position into a slot of the stand about 3-4 cm away from the face of the G.M. counter. Record the counts for 1 min. This is done to find out the number of particles which enter the counter after being scattered by the tray and the blank ring.

   Note that we may need to place three absorber rings at the same time. Therefore, the space between the absorber tray and the GM counter should be sufficient enough to accommodate the three rings of absorber.

   The absorber foil should be placed as near to the counter as possible. This is necessary because some of the β^- particles, while passing through the absorber, not only lose energy but also get scattered to a wide angle. With the absorber placed away form the counter but near the source, some of the particles will be scattered away from the counter and thus be lost, resulting in some loss in counts. This will falsely add to true absorption.

5. Next, place the absorber having the least thickness on the tray and insert it in position. Record counts for 1 min.

6. Repeat step 5 with absorbers of increasing thickness "one by one" till a thickness is reached when all the particles are absorbed. This situation is indicated by fall of counts to the background level. Continue taking readings with at least 5 more thicker absorbers.

   7. Remove the source and the absorber. Record background for 5 min again. Add the readings for background taken under step 2, then divide the total by 10 to get the

background counts per min.

7. Plot count vs. absorber thickness in mg/cm^2 on a semi-log graph paper. Draw curve through these points.

8. Extrapolate the true absorption curve to meet the abscissa. This meeting point gives the range R in gm cm^{-2}.

9. Using this value of R calculate E_β^{max} from Glendenin's and Bleuler and Zunti's relations. Compare the values obtained.

10. Repeat steps 1 to 10 for a ^{90}Sr source.

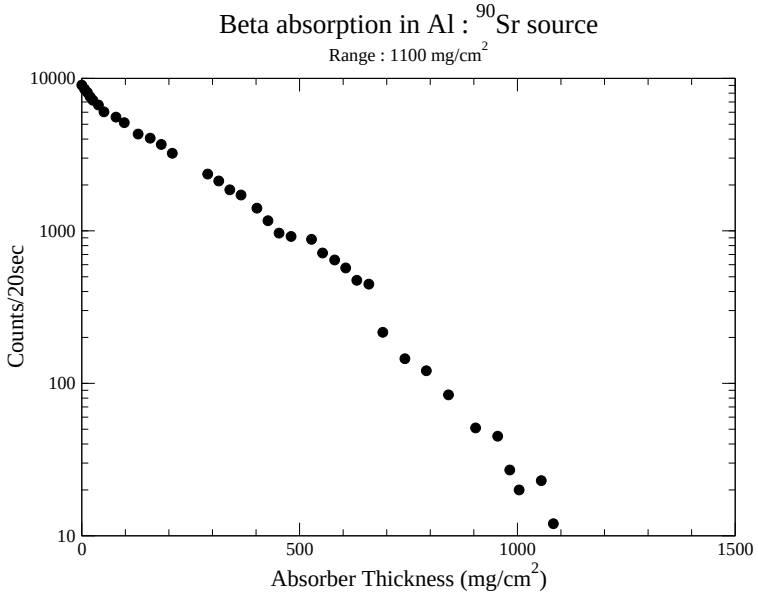

Figure 1.26: Absorption plot for beta particles from ^{90}Sr source in Al. Range of the beta particle is calculated from the intercept on the x-axis.

Fig. 1.26 shows absorption of beta particles from ^{90}Sr source in Al absorber. A range of $R \simeq 1100$mg/cm^2 is obtained from the plot. Using equations 1.49 and 1.50, we have the values 2.275 and 2.208 MeV for beta end-point energy, respectively. These are in good agreement with the standard value of $E_\beta^{max} = 2.280$ MeV.

If this experiment is performed with a β^- source (viz., ^{137}Cs) which also emits γ-rays, a tail will be found (see Fig. 1.27. This happens because these γ-rays (energy = 662keV) are absorbed only by a small amount in aluminum while traveling through a thickness which is enough to completely absorb β^--particles of energy as high as 2 MeV.

11. If the data are plotted in log-scale, the data points due to gamma rays will be linear and can be fitted with a linear function. Contribution due to gamma rays at lower absorber thickness is obtained by extrapolating the fitted curve to lower values (shown by the dotted line in Fig. 1.27). True counts due to β^- particles are then obtained by point to point subtraction (see Fig. 1.28). Plot the data once again after subtraction of counts due to gamma rays to obtain the true absorption curve for β^- particles.

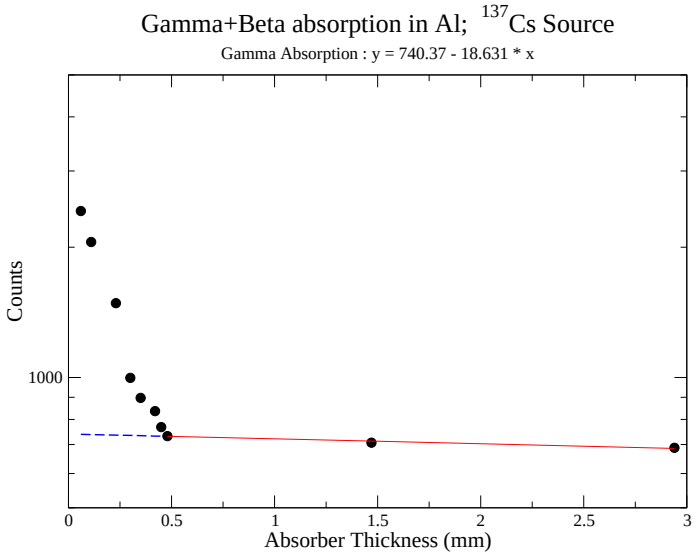

Figure 1.27: Absorption plot for beta particles and gamma rays from ^{137}SCs source in Al. The counts due to gamma rays is fitted with exponential function. The dashed line is extrapolation of the fit to lower thickness.

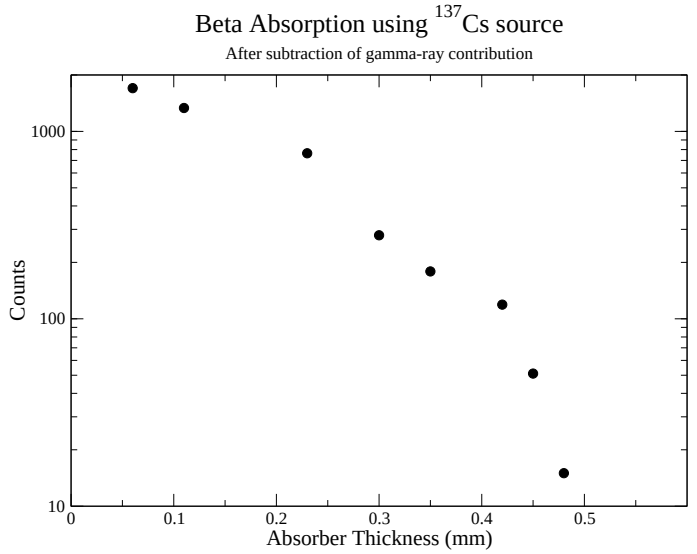

Figure 1.28: Absorption of beta particles in Al. The contribution of 662-keV gamma ray of ^{137}Cs source has been subtracted.

Extrapolate the true absorption curve to meet the abscissa to find R.

From the plot of Fig. 1.28 a range $R \simeq 0.48$ mm which is equivalent to 0.130 mg/cm^2 (density of Al is 2.7 gm/cm^3) can be calculated. The equations 1.49 and 1.50 give maximum beta energy 485 and 510 keV, respectively. The standard value to end-point energy of the beta particle is 514 keV.